Histopathological changes in the Greenshell mussel, *Perna canaliculus*, in response to chronic thermal stress

Joanna S. Copedo[1,2]*, Stephen C. Webb[1], Norman L. C. Ragg[1], Jessica A. Ericson[1], Leonie Venter[2], Alfonso J. Schmidt[3], Natalí J. Delorme[1], Andrea C. Alfaro[2]

[1]*Cawthron Institute, Private Bag 2, Nelson 7042, New Zealand.*

[2]*Aquaculture Biotechnology Research Group, Department of Environmental Science, School of Science, Auckland University of Technology, Private Bag 92006, Auckland 1142, New Zealand.*

[3]*Hugh Green Cytometry Centre, Malaghan Institute of Medical Research, PO Box 7060, Wellington 6242, New Zealand*

*Corresponding author: Joanna.copedo@cawthron.org.nz

Pre-Proof

Abstract

Climate change associated temperature challenges pose a serious threat to the marine environment. Elevations in average sea surface temperatures are occurring and increasing frequency of marine heatwaves resulting in mortalities of organisms are being reported. In recent years, marine farmers have reported summer mass mortality events of the New Zealand Greenshell mussel, *Perna canaliculus,* during the summer months; however, the etiological agents have yet to be determined. To elucidate the role of thermal stress, adult *P. canaliculus* were exposed to three chronic temperature treatments: a benign control of 17°C and stressful elevations of 21°C and 24°C. Eight mussels per treatment were collected each month throughout a 14-month challenge period to identify and investigate histopathological differences among *P. canaliculus* populations exposed to the three temperatures. Histopathology revealed several significant deleterious alterations to tissues associated with temperature and exposure time. Increasing temperature and progression of time resulted in 1) an increase in the number of focal lipofuscin-ceroid aggregations, 2) an increase in focal hemocytosis, 3) an increase in the thickness of the sub-epithelial layer of the intestinal tract and 4) a decreased energy reserve cell (glycogen) coverage in the mantle. Prolonged exposure, irrespective of temperature, impacted gametogenesis, which was effectively arrested. Furthermore, increased levels of the heat shock protein 70 kDa (HSP 70) were seen in gill and gonad from thermally challenged mussels. The occurrence of the parasite *Perkinsus olseni* at month 5 in the 24°C treatment, and month 7 at 21°C was unexpected and may have exacerbated the fore-mentioned tissue conditions. Prolonged exposure to stable thermal conditions

therefore appears to impact *P. canaliculus*, tissues with implications for broodstock captivity. Mussels experiencing elevated, temperatures of 21 and 24°C demonstrated more rapid pathological signs. This research provides further insight into the complex host-pathogen-environment interactions for *P. canaliculu*s in response to prolonged elevated temperature.

Key words

Environmental stress, Greenshell mussel, histopathology, gametogenesis, atresia, *Perkinsus olseni*

1. Introduction

Climate observations have demonstrated the role of climate change on global environmental stressors for more than a decade (Thomas et al., 2004; Mooney et al., 2009). Oceanic environmental challenges as a result of climate change include wider fluctuations in pH, salinity and temperature (Boyd et al., 2014). Not only are elevated average sea temperatures expected (Houghton et al., 2001), but marine heatwaves (MHW) are likely to increase in frequency, particularly in coastal regions (Lubchenco et al., 1993; Houghton et al., 2001; Petes et al., 2007; Filgueira et al., 2016; Smale et al., 2019). Ocean temperatures have already increased by an average of 1.5°C over the past century and will continue rising (Hobday et al., 2016; Tuckett et al., 2017). Marine heatwaves are of particular interest due to correlations between elevated temperature and mass die-offs of marine organisms during the summer period, loosely termed "summer mortalities" (Salinger et al., 2020a). Heatwave-related mortalities have impacted several molluscan populations and aquaculture industries worldwide, with several environmental stressors, including high temperature and pathogens (e.g., *Perkinsus marinus*) being identified as causal agents (Harvell et al., 1999; Garrabou et al., 2009; Rubio-Portillo et al., 2016).

New Zealand's coastal waters host a rich and diverse ecosystem, which is greatly impacted by temperature elevations (Stenton-Dozey et al., 2020; Behrens et al., 2022). In addition to long-term warming of New Zealand's coastal waters, there has been a rise in MHW frequency (Oliver et al., 2017; Salinger et al., 2019; Sutton and Bowen, 2019; Behrens et al., 2022). An

Pre-Proof

unprecedented MHW in the austral summer of 2017/2018 resulted in a mass mortality event of bull kelp (*Durvillea* spp.) in the South Island of New Zealand (Thomsen et al., 2019; Salinger et al., 2020b). As a result of increasing frequency of MHW events, it is likely that sea surface temperature (SST) will exceed thermal optima for local species, resulting in increased detrimental thermal exposure for many marine organisms. Elevated temperatures can significantly affect processes such as, metabolism, reproduction, immune response, and growth (Portner, 2002; Angilletta Jr and Angilletta, 2009; Filgueira et al., 2016; Dunphy et al., 2018). Survival of thermal stress requires a fine balance between cellular response, cell integrity and homeostatic capacity. Furthermore, stress compromises the immune system resulting in disease susceptibility (Trump et al., 1997; Manduzio et al., 2005; Fulda et al., 2010; Carella, 2015; Delorme et al., 2021). When an animal is exposed to sublethal stressors such as increased temperature, reproduction can also be inhibited as energy is reallocated to defence and tissue repair (Michalek-Wagner and Willis, 2001; Petes et al., 2007). In addition, timing of reproduction can be disrupted and result in asynchronicity of spawning and decreased fertilization (Walther et al., 2002; Philippart et al., 2003; Petes et al., 2007). Response to these increasing heatwave events is, therefore, likely to lead to various biological consequences and may even alter phenology and species ranges (Parmesan and Yohe, 2003; Petes et al., 2007; Seuront et al., 2019; Delorme et al., 2021).

The Greenshell mussel, *Perna canaliculus* (Gmelin 1791), is endemic to New Zealand (Jeffs et al., 1999; Alfaro et al., 2001) naturally inhabiting a wide range of temperatures and salinities (Jeffs et al., 1999). It is not only an ecologically and culturally valuable species, but *P. canaliculus* farming is considered the cornerstone of the aquaculture industry in New Zealand (Dawber et al., 2004; Stenton-Dozey et al., 2020). Unlike more mobile species such as fish, mussels have a limited capacity to relocate when conditions, such as increasing seawater temperatures, become unfavourable. Due to this sedentary lifestyle mussels, such as the *P. canaliculus*, have developed effective strategies to minimise the impact when exposed to short term environmental stressors (e.g. de la Ballina et al., 2022). Key strategies include the ability to close their shells thereby reducing contact to the soft tissues, and physiological adaptations such as the development of an effective immune system (e.g. Gosling, 2008; Chong, 2022; de la Ballina et al., 2022). The importance of *P. canaliculus* has prompted various research projects in relation to thermal stress (e.g. Ren and Ross, 2005; Ren et al., 2020; Stenton-Dozey et al., 2020). Effects of acute thermal stressors on *P. canaliculus* have previously been studied

Pre-Proof

to some extent (e.g. Dunphy et al., 2013; Dunphy et al., 2015; Dunphy et al., 2018; Delorme et al., 2020a; Delorme et al., 2021); however, very few studies have focused on the effects of prolonged thermal stress (Ericson et al., 2023). Previous works include recent metabolomic research on *P. canaliculus* during a summer heatwave event and acute, and chronic, heat exposure studies. These have found signs of stress and disruptions to metabolic pathways relating to, for example, energy metabolism and oxidative stress (Li et al., 2020; Nguyen and Alfaro, 2020; Delorme et al., 2021; Ericson et al., 2023). Metabolomic assessments provide a snapshot of the biological response at the time of sampling (Alfaro and Young, 2018), in contrast histology can give insights into cumulative effects on tissues that may develop over time (Costa, 2018). Consequently, this method may provide further insights into the effects of prolonged thermal stress and marine heatwave exposure at the tissue level of *P. canaliculus* in New Zealand as these are largely unknown, as are the etiological agents of thermally mediated mortalities.

Histopathology is an essential tool in the presumptive diagnosis of diseases and mortality investigations as part of health surveillance (Hooper et al., 2014; Knowles et al., 2014; Costa, 2018). It is a bench-mark screening method that can provide a phenotypic anchor point for specific data as it provides tissue-level measures of general, reproductive, and metabolic condition as well as pathogen detection (Bignell et al., 2008; Zannella et al., 2017). In the present study, histopathology, and immunohistochemistry (IHC) were used to elucidate alterations in *P. canaliculus* tissues, as well as presence and prevalence of pathogens, when exposed to prolonged thermal stress. Temperatures were selected based on a summer ambient (17°C SST), present-day high summer temperatures (21°C high summer SST), and a projected high according to a +2.5°C predicted increase (24°C projected summer SST by the year 2100) (Law et al., 2017; Ericson et al., 2023). Identifying alterations to *P. canaliculus* tissue condition and constitution in relation to increasing and prolonged temperature exposure is required to observe the effects of stressors on the tissue structure and architecture. As such this research aims to improve our knowledge on detecting thermal stress and correlation with tissue condition and pathogens. Therefore, providing insights into potential impacts and implications in response to future climate stressors.

2. Methods

Pre-Proof

2.1. Experimental design

Adult *Perna canaliculus* (80 – 120mm shell length, n=1215) were transported from a farm in the Pelorus Sound, Marlborough, New Zealand to laboratories at the Cawthron Aquaculture Park, Nelson, in May 2018. The mussels were weighed (±1g), shell length measured (±1mm) and engraved with identification numbers (Dremel 3000 rotary tool with a 1.6mm round diamond tip). The mussels were then distributed to nine well aerated 100 L tanks (n = 135 per tank) designed for broodstock holding. After 6 weeks of acclimation to the current ambient seawater (16°C ± 2°C), the temperature was increased approximately 0.25° and 1.8°C per day over two weeks depending on temperature treatment until the tanks reached the desired temperatures: 'benign' 17°C, and elevated 21°C and 24°C, with three replicate tanks per temperature (see Figure 1 in Ericson et al. (2023) for the temperature trajectory for each treatment). The control temperature was maintained in three primary header tanks using a heat pump set to 17°C, while the 21°C and 24°C treatment temperatures were obtained by heating the control temperature using titanium and glass submersible heaters. Mussels were continuously fed bloomed algae pond seawater throughout the trial supplemented with a 50:50 combination of monocultured *Tisochrysis lutea* (formerly *Isochrysis galbana*) and *Chaetoceros calcitrans* (250L/day) for a full description of feed and water conditions see Ericson et al. (2023). *P. canaliculus* individuals were weighed (g) and measured (mm) after 2-, 5-, and 10-months exposure. Mortalities were reported daily and immediately removed from the system. The shell lengths of dead animals were measured and recorded to provide an indication of growth to mortality. Weighing was not performed due to loss of tissue mass through rapid decay. This rapid decay also prevented harvest of dead specimens for histopathology.

2.2. Water quality sampling

Seawater flows (2.5 ± 0.5L/min) were measured twice weekly and adjusted as required. Water quality parameters (dissolved oxygen, temperature, pH and chlorophyll-*a*) were measured throughout the trial and reported within Ericson et al. (2023).

2.3. Histopathology

Eight *P. canaliculus* per temperature treatment (17°C, 21°C and 24°C) were randomly collected across replicate tanks each month and prepared for histopathological assessment. An additional 10 mussels per temperature, were collected at 4 time points throughout the trial (labelled as month and letter B in Table. 1).

Table 1. Sampling numbers and collection months for each of the temperature treatments over the 15 months (July 2018 – Sept 2019). A fixation issue at month 3 resulted in a lack of individuals for the histology assessment. Thus, month 3 is represented graphically but was not included in the statistical analysis. Month 2B was the initial sampling, where all mussels were at 17°C, prior to raising the mussels to the desired temperature achieved by month 3 (None available (NA)). At month 15B there were no mussels left in the 24C treatment to sample (NA).

		Sampling month and date															
		2B	**3**	**4**	**5**	**6**	**6B**	**7**	**8**	**9**	**10**	**11**	**11B**	**12**	**13**	**14**	**15B**
				2018				**2019**									
		21 Aug	24 Sept	19 Oct	19 Nov	01 Dec	06 Dec	02 Jan	25 Feb	03 April	02 May	04 Jun	11 Jun	10 Jul	05 Aug	30 Sept	15 Oct
Temperature	**17°C**	15	1	8	8	8	10	8	8	8	8	8	10	8	8	8	18
	21°C	NA	3	8	8	8	10	8	8	8	8	8	10	8	8	8	18
	24°C	NA	0	8	8	8	10	8	8	8	8	8	10	8	8	4	NA

Tissues were removed intact from the shell and sectioned as shown in figure 1. The 5mm sectioned samples (mantle, gill, kidney, digestive gland, mid-gut, muscle, and nervous tissue) were placed into histological cassettes and fixed in a 4% formalin solution (1:9 v/v, 37% formaldehyde: 0.35µm filtered seawater). The samples were left in the 4% formalin solution for 48 hours before being transferred to a 70% ethanol solution (Howard, 2004). Samples were embedded in paraffin wax, sectioned (3-5µm) using a rotary microtome and stained using routine hematoxylin and eosin (H&E) (Howard, 2004).

Pre-print

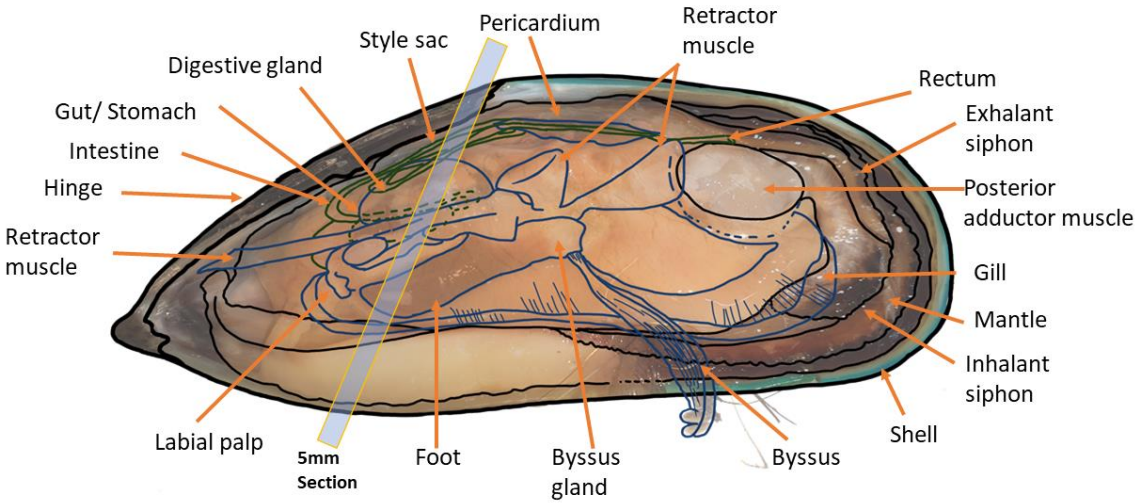

Figure 1. Greenshell mussel (*Perna canaliculus*) general anatomy depiction. Rectangular window indicates the location of the 5mm histology section. This section was selected to maximise chances of acquiring all tissue types, including midgut, digestive gland, gill, gonad (mantle) and muscle.

2.3.1. Tissue Analysis

Histological observation under a light microscope (Olympus BX40), at a magnification of x40 to x1000, was conducted on a range of tissues, assessing tissue-specific alterations by scoring semi-quantitatively and quantitatively as explained below in sections 2.3.2 to 2.3.4.

2.3.1.1. Gill and digestive gland scoring

The gill and the digestive gland were assessed at x200 and x400 magnification, then a score of tissue quality was devised based on structural deviations from those seen in mussels sampled on arrival (Baseline: month 2). The gill and digestive gland grading criteria were generalised and adapted from (Kim et al., 2006) and (Perez-Cebrecos et al., 2022), whereby 0= normal tissue and no obvious changes, 1= ‘mild’: minor alterations, 2= ‘moderate’: up to half of the organ affected and 3= ‘severe’ alterations with marked disruption to tissue architecture. Tissues were graded at each timepoint between the three temperatures (17°C, 21°C and 24°C) and then compared across time (16 months).

2.3.1.2. Mantle and connective tissue scoring

Pre-proof

196 The mantle tissues were graded using four subjective semi-quantitative criteria, each graded
197 from least to most severe: 1) the level of ceroid material found in the section (implicating
198 oxidative stress or previous immune response, for this research ceroid and lipofuscin are
199 considered together), 2) the level of focal hemocytosis (nodule or inflammatory capsule),
200 indicative of an immune response (Table 2; Fig. 4), 3) the level of storage cell material in the
201 mantle, and 4) the width of the subepithelial layer between the gut and the digestive tubule
202 tissue (Table 3; Fig. 5). These scores were developed to assist with the identification of a stress
203 or an immune response to increasing temperature, as well as to help standardise interpretation.
204 The average scores of each of the four criteria for each temperature were plotted against time
205 in a heat map table to detect changes in each related to their respective criteria.

206 Table 2. Semi-quantitative scoring of level of ceroid material and focal hemocytosis from least
207 severe (1) to most severe (4). Criteria are similar to the grading scale of Carella et al., (2015)
208 and Bignell et al. (2008) and specific illustrations are located in the results section..

Score	Ceroid level criterion	Focal hemocytosis level criterion
0	No ceroid material observed	No hemocytosis alterations observed
1	Low level ceroid, focal alterations observed across tissues	Low level focal hemocytosis alterations observed across tissues
2	Moderate level of multifocal ceroid alterations observed across tissues	Moderate level multifocal hemocytosis alterations in multiple tissues
3	Severe level of multifocal ceroid alterations across tissues	Severe multifocal and hemocytosis alterations
4	Extensive diffuse ceroid accumulation in multiple tissue types	Extensive hemocytosis diffusely distributed across multiple tissue types

209

210

211 Table 3. Semi-quantitative scoring of level of storage cell material (glycogen) and gut
212 subepithelial thickening from least severe (1) to most severe (3). A score of 3 for storage cell
213 coverage indicates glycogen rich mantle tissue whereas a score of 1 for the gut is indicative of
214 healthy gut performance, with low numbers of hemocytes around the gut epithelial layer.

Score	Storage cell (Glycogen) coverage criterion	Gut subepithelial layer extent criterion
0	No storage cells observed	None observed (no hemocytes observed around the epithelium).
1	Light coverage of storage granules in the mantle tissue.	Normal thickness the width of the gut epithelium ≤ width of the epithelium.

2	Moderate coverage of storage granules in the mantle tissue.	Thickness greater than thickness of the gut epithelial layer ≤ 2x thickness of epithelium.
3	Full coverage of storage granules in the mantle tissue	Thickness greatly increased expanding into the digestive tissue greater than thickness of gut epithelial layer (Abnormal).

215

216

217 **2.3.1.3. Immunohistochemical detection of HSP70 in gill and gonad: A preliminary**
218 **investigation**

219 Three paraffin blocks prepared from mussel tissues before temperature exposure (month 2b)
220 and 3 blocks after temperature acclimation (month 4) were selected for preliminary assessment
221 of HSP70 as a potential heat stress marker. A 4µm section was obtained from the paraffin
222 blocks as processed and described in section 2.3. The paraffin section was then mounted on to
223 a microscope glass slide. This section was then dewaxed, hydrated, and processed through a
224 heat-mediated antigen retrieval procedure for 5 minutes at 120°C. The prepared slides were
225 stained using an indirect antibody approach with a primary monoclonal antibody reactive to
226 HSP70 (MA3-006, Invitrogen) used at a concentration of 1:200. A complementary secondary
227 antibody conjugated with Alexa fluor 647 (A32728, Invitrogen) was used at a concentration of
228 1:1000. DAPI (0.2 µg ml^{-1}) was then used as a counter stain to highlight the cellular nuclei.
229 Sections were mounted using an aqueous mounting media and 22x50 mm (1.5 H) cover slip.

230 Slides were observed under an inverted microscope (IX83, Olympus, Tokyo, Japan) equipped
231 with a laser scanning confocal head (FV3000, Olympus, Tokyo, Japan), using a 405nm (50
232 mW) and a 640nm (40mW) laser line, and Fluoview FV31S-SW software (version 2.3.2,
233 Olympus Corp.). Images of gill and gonad tissue were acquired using the UplanSApo 20x N.A.
234 0.75 objective and a confocal aperture of 125 µm. These acquisition conditions were
235 established according to Nyquist sampling criterion and acquired signals that fulfil the Rose
236 criterion for signal-to-noise ratio in all the marker channels (Pawley, 2006). Images were
237 collected using the following emission filter configuration for each fluorophore: DAPI (430-
238 470nm), AF647 (650-700nm). Image visualisation and formatting was performed using ImageJ
239 (Schindelin et al., 2012).

240 **2.3.1.4. Reproductive staging**

Gonad development scoring proceeded using the following system similar to Kennedy (2010), Alfaro et al. (2001) and Buchanan (2001) (Table 4). Stage definitions were altered to include maturity of the oocytes as well as mantle coverage. Females and males were scored based on the criteria of stages and given a numerical gonad index value using microscopy (Table. 4). The frequency or proportion at each stage was plotted for visual representation. The gonadal index (GI) was then calculated based on formulae by King et al. (2009), Galinou-Mitsoudi and Sinis (1994), Buchanan (2001) and Alfaro et al. (2001), whereby GI (Gonad index) is determined by the average rank, or score, of the population. A GI of 0 is indicative that the population is closer to the resting phase and a GI approaching 3 the population is close to full maturity. Percent follicle coverage (FC) within the mantle tissue was estimated by eye followed by image analysis. Area analysis was conducted on the 25 females identified within this trial using cellSens™ software (Olympus cellsens Standard 3.1 [build 21199] on an Olympus BX53 compound) to validate the estimates. To validate the percent follicle coverage the area of the frame was recorded then a free-form polygon was used to define the cross-sectional area of each follicle contained within the frame. The percent area coverage was then calculated. The values were then fitted to a regression and compared with the estimates. Estimates by eye were developed to be used for routine determination in a commercial aquaculture setting where image analysis is not always possible.

Table 4. Histological criteria of seven stages and the associated gonad index score for the reproductive condition of *Perna canaliculus.*

Pre-Print

Stage	Gonad index score	Description	Male	Female
Resting	0	Sex indeterminable. Resting or inactive some basal cells and/or very early precursors. Good coverage of storage reserve cells in mantle (glycogen).		
Early	1	Gametogenesis has begun and small germinal cells are present. Follicles 500µm or less in diameter.	Spermatogonia inside follicles along the wall. Some spermatozoa are visible.	Oogonia line follicle wall, oocyte nuclei large attached to wall by cytoplasmic stalk
Late	2	Follicles become larger in size; 50% of follicles equal to, or larger, than medium size and/or both sexes have the potential to spawn and produce 50% or less of their mature sperm when force spawned. Follicles 500µm or more in diameter.	Concentric layers of spermatogonia, spermatocytes and spermatids. 50:50 Precursor to mature cell ratio.	Oocytes accumulate yolk and some mature oocytes are free and/or 50% distribution of precursor cells to mature oocytes.
Ripe	3	Mantle nearly full, with at least 80% coverage of the mantle, follicles are large (1000µm or more) and/or development of gonad is as follows for males and females.	Mantle filled and follicles show <10% precursor cells and with up to 50% of follicles with mature sperm converging in the centre but still dense.	Most oocytes at maximum size and mostly free from the wall, some small loss of oocytes.
Spawning	2	Release of gametes has begun, spillage of loose gametes evident upon histological sectioning. Evidence of a reduction in gamete density within follicle. Less than 80% atresia observed.	Dense band of ripe spermatozoa; greater than 80% spermatozoa converging in the centre with some follicles showing a loss in density.	Ripe oocytes present with a reduction in density of gametes in the centre of the follicle. Very few precursor cells (<10%).
Redevelopment	1	Follicles reduced in size and do not take up all the mantle area, remaining oocytes arranged loosely with new oocytes visible.	Dense band of ripe spermatids give rise to new lamellae, with gaps still present; very few follicles with phagocytosis developing (less than 50%).	Some atresic debris as well as phagocytes, but phagocytes are not affecting the new oocytes.
Spent	0	Follicles either empty or collapsing and degenerate amoebocytes/ phagocytes attack unspawned material, autolysis. Lumen filled with debris, atresia, and phagocytosis. Residual gametes will be broken down.	Phagocytes attack unspawned sperm.	Phagocytes clearing debris and follicles display greater than80% oocyte atresia.
Atresia		Autolysis, degradation, and reabsorption of oocytes. Includes cytoplasmic discolouration and darker staining, irregular jigsaw shape, retraction, and detachment of the cell membrane. Lysing of the cell membrane, oocyte contents spill into follicle. Can occur at any stage.		
Phagocytosis		Phagocytes clear unspawned gametes: the follicle will have cellular debris with some ceroid material visible. Can occur at any stage.		

Pre-Proof

Preliminary investigations of female gonad status and indications of presence of atresic oocytes (defined in Table. 4) resulted in further analysis of the oocyte condition. Three micrographs were taken of the gonad and mantle tissue for each female at 20x using an Olympus BX53 compound microscope and cellSens imaging software (Olympus cellsens Standard 3.1 [build 21199]). Oocytes in each of the micrographs were then quantitatively analysed using methods by Chérel and Beninger (2017). Quantification of the oocytes was performed using stereological counts and oocytes allocated to 3 groups, immature (I) (attached to follicle (acinal) wall; stalked), mature (M) (detached from follicle wall) and atresic (A) (Fig. 2). The three counts were then averaged and recorded to produce a single value per category for each female and the importance of atresia was calculated using the following by Chérel and Beninger (2017):

1) Percent atresia (PA) $= \frac{\mathrm{A}}{\mathrm{I+M+A}} * 100$

2) Percent mature (PM) $= \frac{\mathrm{M}}{\mathrm{I+M+A}} * 100$

3) Percent immature (PI) $= \frac{\mathrm{I}}{\mathrm{I+M+A}} * 100$

4) Atresic impact (AI) $= \frac{\mathrm{PA}}{\mathrm{PA+PM}} * 100$

The atresic impact was determined to be the minimum impact of atresia on the oocytes whereby the fate was known (i.e., spawned as healthy oocytes and fate known). Health of immature oocytes was yet to be determined and could either develop into healthy oocytes or become atresic (Chérel and Beninger, 2017).

Pre-Proof

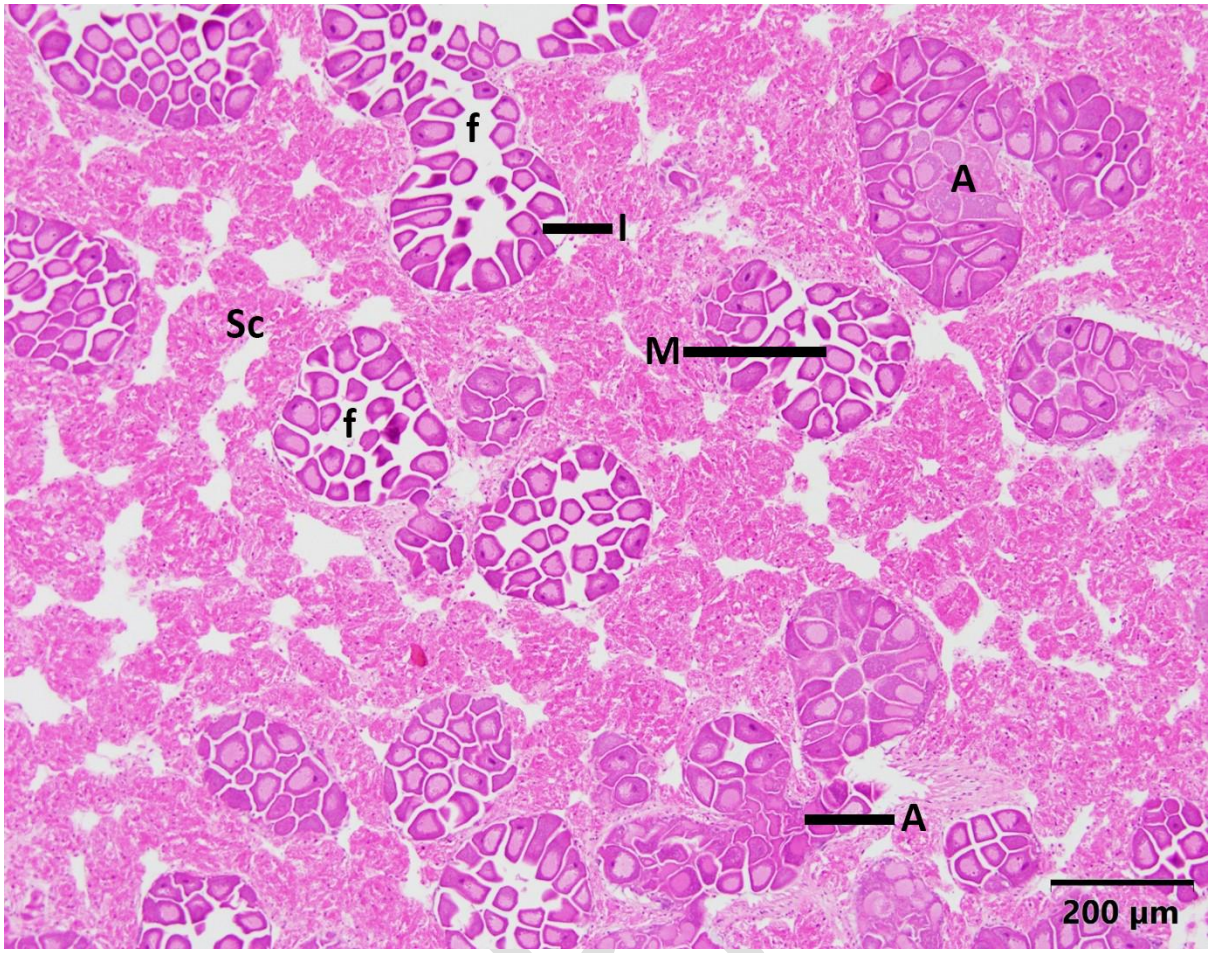

Figure 2. Female gonad stained with H&E indicating stages of oocytes immature (I), mature (M), atresic (A) within the follicles (f) and glycogen rich mantle storage cell (Sc).

2.3.2.3. Pathogens

Presence/absence of parasites was recorded and presented as proportion of population prevalence. The apicomplexan-X (APX) and *Perkinsus olseni* were the most prevalent and, as such, were investigated further (Fig. 5). The intensity of APX and *P. olseni* were scored using adapted methods from Hine (2002), Kim et al., (2006) and Suong (2018) (Table 5). The section was screened at x200 to identify cells, x400 and x1000 magnifications were then used for further identification. Following the histological identification of *P. olseni*, a selection of processed blocks was sent to the NZ Ministry for Primary Industry National Animal Health Laboratory and subjected to PCR screening using standard and specific primers to confirm diagnosis.

Table 5. Two parasites, APX and *Perkinsus olseni*, were scored using a 0 – 5 grading scale, where 0 indicated no parasites were observed and 5 is a severe level of parasites was observed (Hine, 2002; Kim et al., 2006; Suong et al., 2018).

Score	*APX*: Criterion	*Perkinsus olseni*: Criterion
0	No parasites were observed in the tissue section.	No parasites were observed in the cross-section.
1	Low: Parasite difficult to detect <10 APX zoites were present in the tissue section after extensive search.	Low: <10 *Perkinsus* cells observed in tissues after extensive searching. For the purpose of this scoring rosette- stage groups were considered as 1.
2	Moderate: APX zoites were present in the tissue section and detected in small groups. Occasionally associated with ceroid material.	Moderate: *Perkinsus* cells were observed in tissues and more easily identified.
3	High: APX zoites were more easily detected, developing multiple moderate to large lesions of APX zoites and in most cases associated with ceroid.	High: *Perkinsus* cells observed to be distributed in multiple tissues *Perkinsus* cells. No lesions observed.
4	Heavy: APX zoites abundant in most tissues developing large lesions.	Heavy: *Perkinsus* cells abundant in most tissues, developing lesions.
5	Severe: APX zoites abundant with high tissue congestion and connective tissue destruction.	Severe: *Perkinsus* cells abundant in most tissues, developing large and abundant lesions.

2.4. Statistical analysis

Statistical analyses were conducted using R version 4.0.3 (R Core Team, 2021) with the R studio interface (RStudio Team, 2021). Histology data were analysed using both temperature and time as explanatory factors. Quantitative data (follicle coverage and atresia) were checked for normality and homogeneity of variance using the Shapiro-Wilks and Levene's tests, followed by analysis using ANOVA. The atresia data were non-normal and unbalanced due to the lack of female representation in each category. However, ANOVA Type II sum of squares at the 0.05 level was used as the data met the requirement for homogeneity of variance (Quinn and Keough, 2012). Analysis of the semi-quantitative data (hemocytosis, ceroid material, mantle reserve cell, gut subepithelium and gonad index) was performed using a Generalised linear mixed effect model in the MCMCglmm package (Hadfield, 2010). Tank number was included as a random effect for the MCMCglmm however was tested and excluded from the other analyses. Binomial general linear models were performed on the pathogen (APX and *P. olseni*) prevalance data. Ridge penalizers were added prior to the estimates to increase data 'sensibility' if the differences between the responses were deemed as "perfect" (Cule and Frankowski, 2021). A p value < 0.05 was considered statistically significant.

3. Results

3.1. Water quality and survival

Pre-Proof

On initiation of the trial, once seawater had reached the desired temperature, the treatments were maintained at that temperature. A logistical issue with the temperature system occurred in the 21°C and 24°C treatments during month 10 of the experiment and the temperature dropped to 17°C for 2 weeks (see Ericson et al., 2023). Analysis of mussel tissue alternations did not reveal obvious effects from this technical difficulty. Temperatures were slowly increased back to 21°C and 24°C once the system's malfunctioning was repaired. The dissolved oxygen and pH levels remained stable through the trial (Table 6).

Table 6. Water quality parameters (mean ± standard error (SE)) measured throughout the experiment.

	Desired temperature		
Water parameter	**17°C**	**21°C**	**24°C**
Temperature (recorded)	17.9 ± 0.5°C	21.2 ± 1.0°C	23.2 ± 1.6°C
Dissolved oxygen	92.6 ± 1.3%	90.5 ± 0.3%	90.6 ± 1.3%
pH	8.14 ± 0.01	8.12 ± 0.01	8.13 ± 0.01

Survival was significantly impacted by chronic temperature exposure to 24°C, and a mortality began at month 5 of the trial until a 100% mortality was reached at month 15. At 17°C and 21°C, survival at completion of the trial was at 94% and 90%, respectively (see complementary study presented by Ericson et al. (2023) for further details). No individuals were available for sampling from the 24°C treatment in the final month of the trial.

3.2. Tissue condition

3.2.1. Gill and digestive gland architecture

There were statistically significant histological differences in the appearance of the digestive gland tissue (Temp*Month p=0.008) and the gills (Temp*Month p=<0.001) in mussels among the three temperatures. There was an observable histological trend towards degradation in tissue architecture in the digestive gland and the gill condition of the mussels kept at all temperatures over time. These effects were only subtly different15or the digestive gland there were individuals with 1) an increase in the intracellular spaces in the epithelium, which took on an increasingly thin and lacey appearance, 2) minor epithelial atrophy, and 3) epithelial sloughing in a few individuals, as well as a minimal increase in the amount of interstitial space

Pre-Proof

between the tubules as time progressed (Fig. 3a and b). For the gills, there were individuals with some minor lifting between the chitin layer and the epithelium, increased cell separation, minor hemocyte infiltration, in some cases loss of cilia and an accumulation of ceroid material as time progressed (Fig. 3c and d).

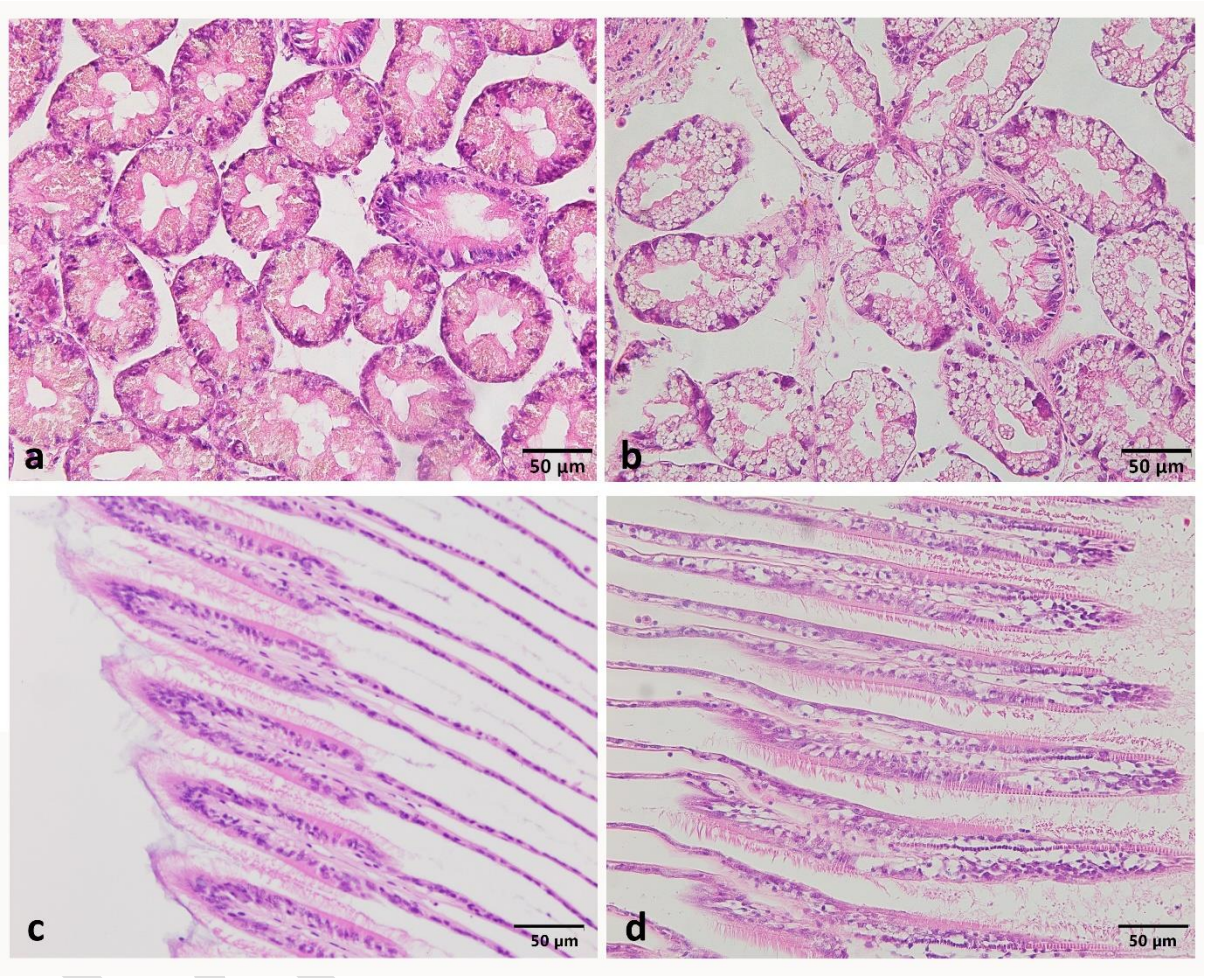

Figure 3. General alterations to digestive gland tissues at trial start and trial end A) normal digestive gland at trial initiation (graded as 0) B) altered digestive gland after 14 months at 24°C with expanded intracellular spaces (graded as 2). *Perna canaliculus* gill prior to acclimation to the temperature treatments C) Healthy gill filaments (graded as 0) and D) Gill filaments after 14 months with alterations to the gill architecture and no loss of cilia as described in section 2.3.1.1. (graded as 2). Scale = 50µm.

3.2.2. Mantle and connective tissue

Semi-quantitative criteria of ceroid granules, focal hemocytosis, mantle storage cell coverage and the extent of the sub-epithelial layer of the gut indicate that the differences between the

363 temperature treatments were linked to the month and were amplified over time (chronic time
364 factor) (Table. 7).

365

366

367 Ceroid material was present in the majority of individuals and increased with both temperature
368 and time (Temp*Month p<0.001). Focal hemocytosis increased in intensity (, p <0.001). with
369 increasing temperature and was amplified over time ((Temp*Month p=<0.001). There was a
370 decrease in the coverage of the mantle storage cells which was also influenced by exposure
371 time (Temp*Month p<0.001). The subepithelial layer of the gut increased in thickness,
372 extending into the digestive tubule tissue increasingly over time (Temp*Month p<0.001)
373 (Table. 7). In some individuals, the thickness was extensive and displaced the digestive tubules,
374 resulting in the appearance of higher numbers, and increased density, of hemocytes.

375 Table 7: Heatmap of the semi-quantitative levels of ceroid material, focal hemocytosis, mantle
376 storage cell coverage and the thickness of the subepithelial layer of the gut. Sampling month 3
377 had fixation issues and, as such, only had an n = 1 at 17°C and n =3 at 21°C; no samples were
378 available for the 24°C treatment. Sampling months 4 to 15 had n = 8 at 17°C, n = 8 at 21°C
379 and n = 8 at 24°C for each sampling month (Table. 1). Where no data were collected, cells are
380 blacked out.

381

Impact level

No impact Increasingly impacted

		Sampling month															
		2B	3	4	5	6	6B	7	8	9	10	11	11B	12	13	14	15B
Ceroid granules	**17°C**	0.9	1.0	0.8	0.4	1.1	1.3	1.2	1.2	1.3	1.4	1.5	1.1	1.1	1.2	1.1	1.6
	21°C		1.0	0.6	0.9	1.0	1.3	1.1	1.4	1.0	1.6	1.3	1.0	1.5	2.5	2.1	1.8
	24°C			1.0	1.3	1.3	1.2	1.3	1.7	1.9	2.5	2.1	2.6	2.8	3.0	2.8	
Hemocytosis	**17°C**	0.3	0.0	0.1	0.1	0.4	0.3	0.2	0.7	0.8	0.6	0.9	0.7	0.4	0.8	0.5	0.9
	21°C		0.0	0.0	0.1	0.3	1.0	0.3	0.7	0.3	0.6	1.0	0.9	0.9	1.4	1.5	1.2
	24°C			0.0	0.0	0.6	0.2	1.3	1.3	1.1	2.4	2.1	2.2	2.0	2.2	2.0	
Mantle storage cell	**17°C**	1.9	3.0	2.3	2.1	1.9	2.4	2.3	2.2	2.0	2.9	2.3	2.8	2.6	2.2	2.0	2.7
	21°C		2.7	2.3	2.1	2.0	2.2	2.1	2.0	2.0	2.8	1.8	2.8	2.1	1.7	0.4	1.9
	24°C			2.1	1.9	1.9	2.5	2.0	2.0	2.0	1.7	2.1	1.6	1.4	1.8	0.5	

Pre-Proof

sub-epithelial gut layer																
17°C	1.1	1.0	1.0	1.0	1.1	1.0	1.2	1.8	1.7	1.8	2.1	1.9	1.6	1.6	1.6	1.5
21°C		1.0	1.1	1.2	1.2	1.5	1.4	1.8	2.0	1.7	2.7	2.2	2.1	2.0	2.0	1.5
24°C			1.1	1.1	1.2	1.3	1.1	1.8	2.0	2.3	2.4	2.4	2.3	2.4	2.1	

382

383

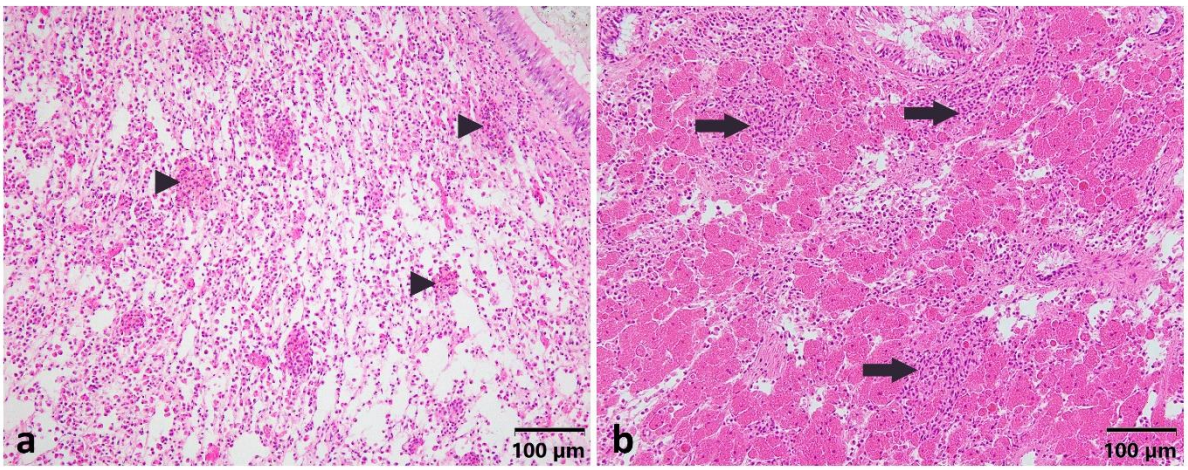

384

385 Figure 4. Ceroid level and the focal hemocytosis level 3. a) Severe level (score 3) of ceroid
386 material, multiple accumulations observed (arrowhead) b) Severe level (score 3) of focal
387 hemocytosis with multiple patches throughout the mantle tissue.

Pre-Print

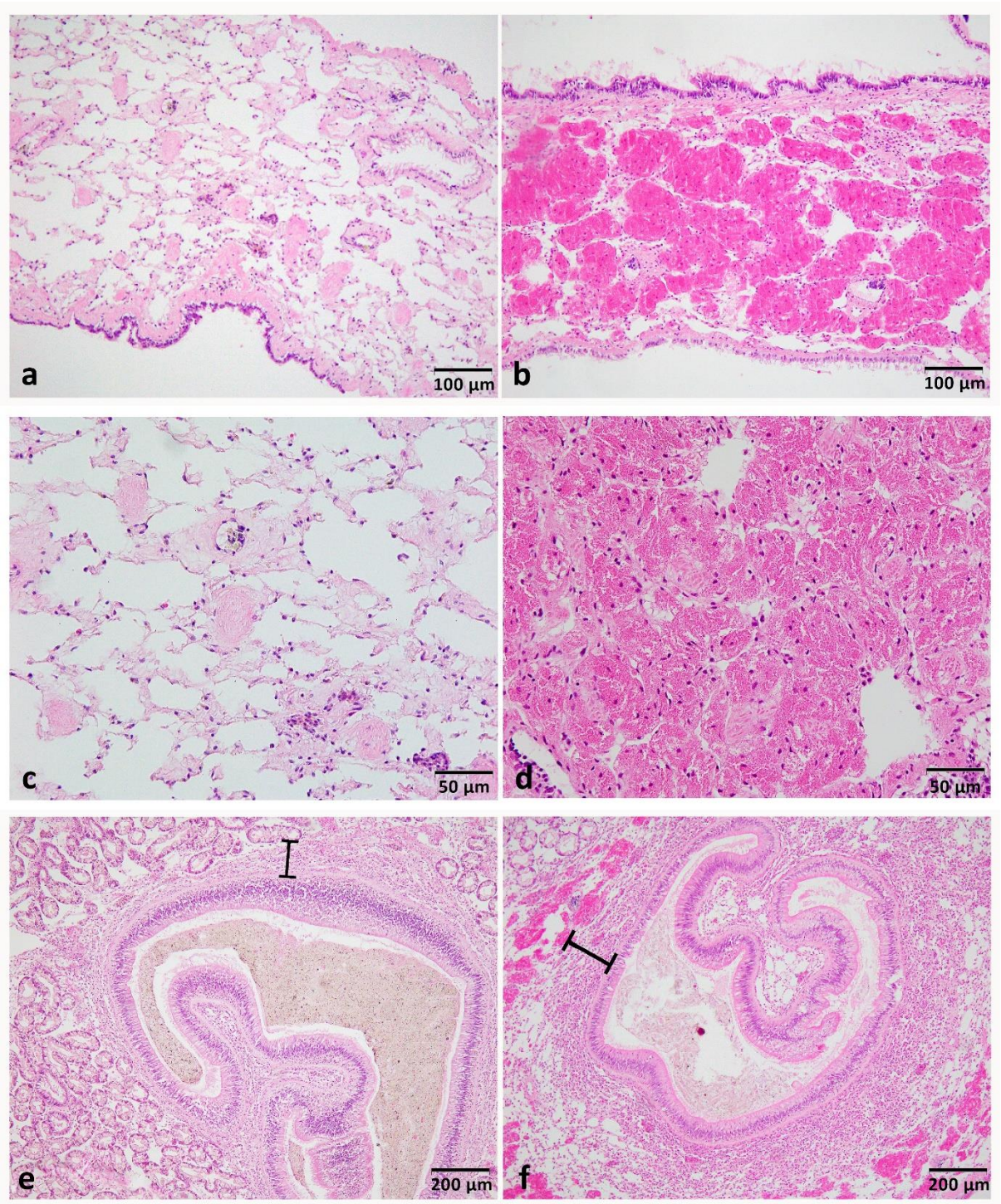

388

389 Figure 5. Mantle storage cell coverage and the subepithelial extent or thickness. a) Mantle
390 tissue with a score of 0 no glycogen cells (granules) observed higher levels of hemocytes and
391 connective tissue visible. b) Mantle tissue with a score of 2 with some patches of no storage
392 cell tissue. c) Zoomed in mantle tissue of image a, only connective and some musculature
393 tissue, with no visible glycogen granules. d) Zoomed in mantle tissue of image b showing
394 densely packed storage cells e) Subepithelial layer of the intestine score of 1, low level of

hemocytes surrounding the epithelial layer of the intestine f) Subepithelial anomalous thick layer (score of 3) around the intestine extending into the digestive tubule region, indicating increased number of hemocytes surrounding the intestine Black line indicating subepithelial layer

3.2.3. Immunohistochemical exploration of HSP70 in gill and gonad: A preliminary investigation.

HSP70 presence in the gills appears to be localised to the epithelial cells at the frontal lateral edge of each filament (Fig. 6 b, c, and d). The gill tissue suggested an increase in HSP70 protein abundance with temperature in the 'benign' and elevated one-month post-temperature acclimation. At this stage HSP70 proteins were not observed in the ambient (17°C ± 2°C) samples prior to the temperature increase for the experiment (Fig. 6 a).

HSP70 was suggested to be visible at elevated temperatures in both male and female gonads. HSP70 in males appeared to be localised to spermatogonia and spermatocytes (Fig 6 e and f). Female oocytes were highly abundant with HSP70 some oocytes displayed dense "patches" with elevated temperatures (Fig. 6 g and h).

Pre-Proof

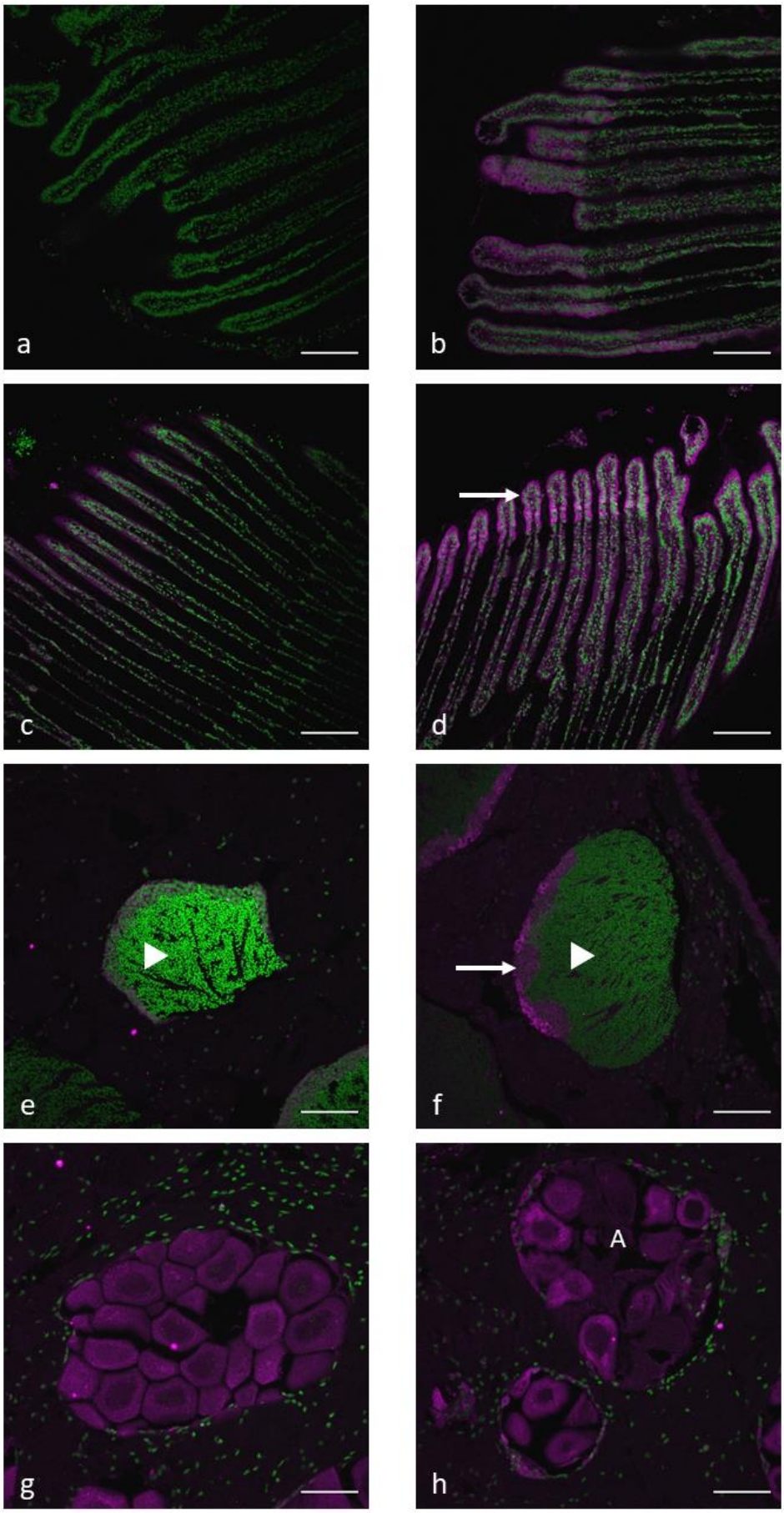

412

Figure 6. Preliminary investigations show the presence of HSP70 in gill and gonad tissue determined by immunohistochemistry. a) gill tissue in 17°C temperature at month 2 prior to the temperature elevation. Images b, c and d correspond to mussels that had been exposed for 1 month at 17, 21 and 24°C, respectively. Male reproductive follicle HSP70 (magenta) detected to be associated to spermatogonia and spermatocytes, green is the mature sperm cell at 2 temperatures 1-month post-temperature increase e) 17°C and f) 21°C. Female reproductive follicle at 2 temperatures 1-month post-temperature increase g) 17°C and h) 21°C with increased atresic oocytes (A). Magenta (arrow) is the HSP70, and green (arrowhead) is the nuclear material. Images A - D Scale bar= 100µm, Images E – H Scale bar= 50µm.

3.3. Reproductive tissue

Reproductive condition and gametogenesis appeared to have regressed over time, with much of the population in either the spent or resting phase of gametogenesis by month eight. Initial observational patterns suggest a natural decline (month 3 to 5 [21°C] and 6 [17°C]) from mature individuals to the rest and spent phase, but no initiation of gametogenesis after the rest phase (Fig. 8). There was no significant difference in gonadal development among the treatment temperatures ($p=0.87$), nor in the interaction with month ($p=0.49$) (Fig. 7).

Pre-Proof

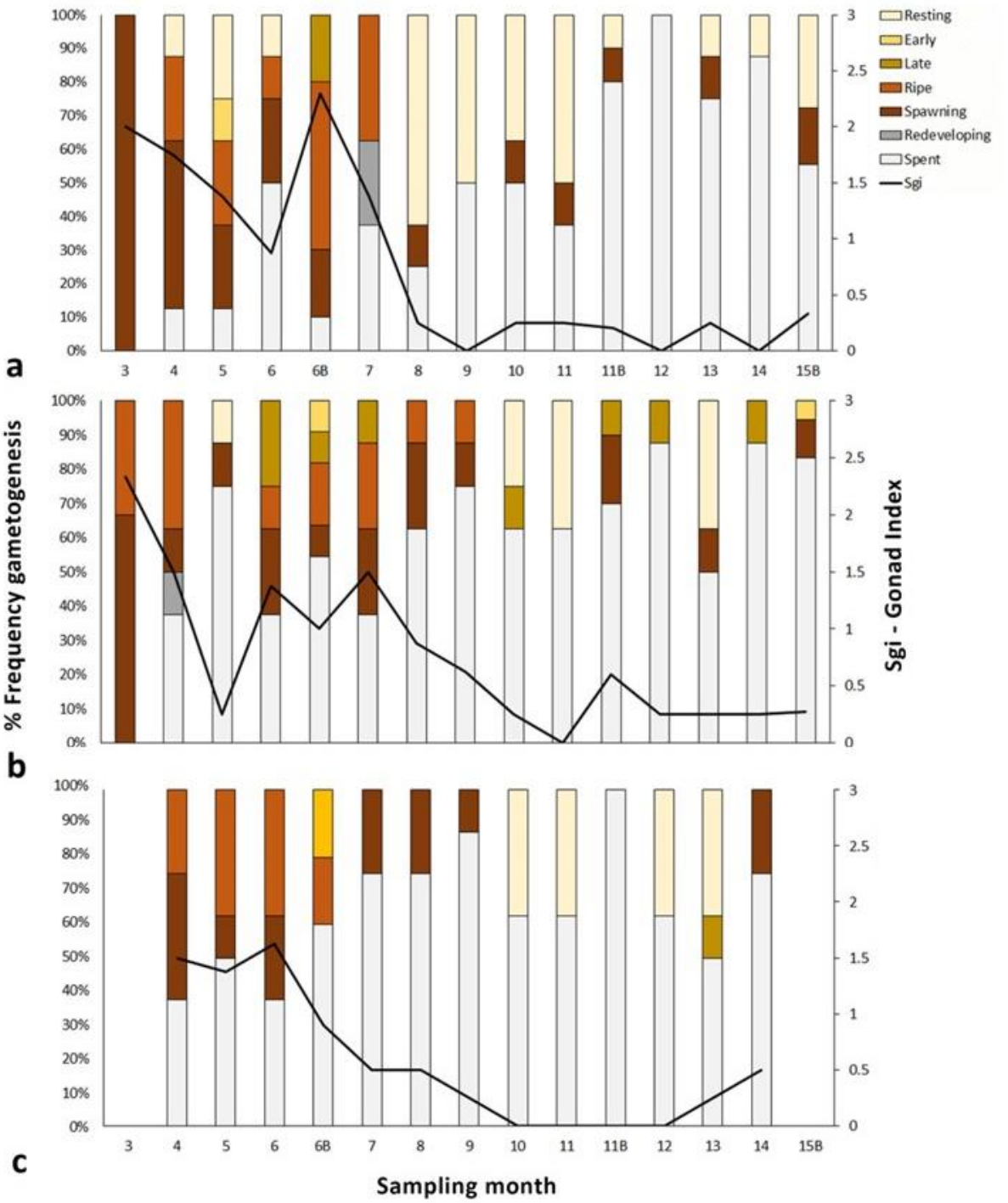

Figure 7. Gonad condition (proportion of sampled individuals in each development stage and overall gonad index) over 14 months exposure to a) 17°C, b) 21°C and c) 24°C. No data were collected at month 3 or 15B for 24°C.

There was no difference in the percent coverage of the follicles between the three temperatures ($p > 0.05$). Visual estimates of coverage correlated with objective image analysis quantification

with an R^2 value of 0.93. The female gonad tissue displayed various anomalies, particularly in the spent category: 1) dilated follicles post-spawning, 2) dilated follicles with increased levels of atresic debris, 3) increased numbers of follicles with atresic oocytes and some phagocytosis, and 4) follicle regression and atrophy (Fig. 8).

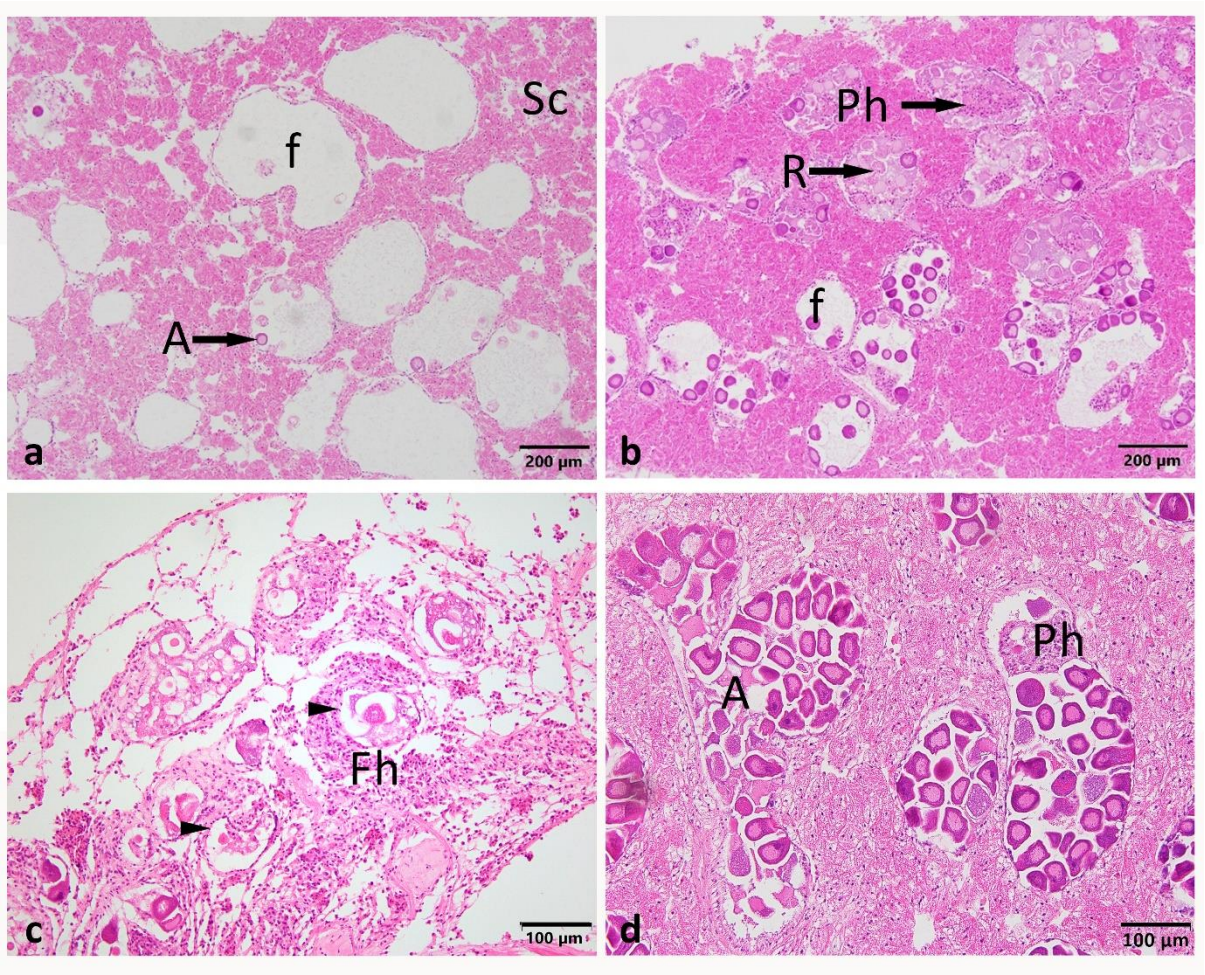

Figure 8. Female reproductive tissue (mantle) showing: a) anomalous dilated post-spawning follicle (f), b) dilated follicles with high levels of atresic debris, c) female mantle tissue with low levels of storage cell (glycogen (Sc)), regressing and atrophying follicles (Arrow) and focal hemocytosis (Fh) from a female in the 24°C treatment, d) full follicles with high level of atresic oocytes (A), residual oocytes (R), and phagocytosis (Ph) within the follicle.

Due to the under-representation of females as a result of the majority of the sexes being indeterminate across the three temperature treatments throughout the experiment, only temperature was used as a factor, and female gonad images from each month were pooled. No significant differences were observed among average proportion of immature oocytes ($F_{(3, 117)}$=0.75, p=0.53), mature oocytes ($F_{(3, 117)}$=0.85, p=0.47), atresic oocytes ($F_{(3, 117)}$=0.3,

p=0.82), and atresic impact ($F_{(2, 109)}$=0.4, p=0.76),.The average proportion of oocytes showing atresia, as well as overall atresic impact was observed to be high across the 17°C, 21°C and 24°C temperatures (62% ± 4.1, 58% ± 4.3, 60% ± 5.8 and 74% ± 3.3, 78% ± 2.9, 75% ± 5.2, respectively (mean percent ± SD)).

3.4. Pathogens

There were several parasites detected in the *P. canaliculus* tissues. These included various unidentifiable ciliates and copepods, as well as a low prevalence of *Paravortex* and *Endozoicomonas* (Table. 8). The two most significant parasites observed were APX (Fig. 9a) and *Perkinsus olseni* (Fig. 9b).

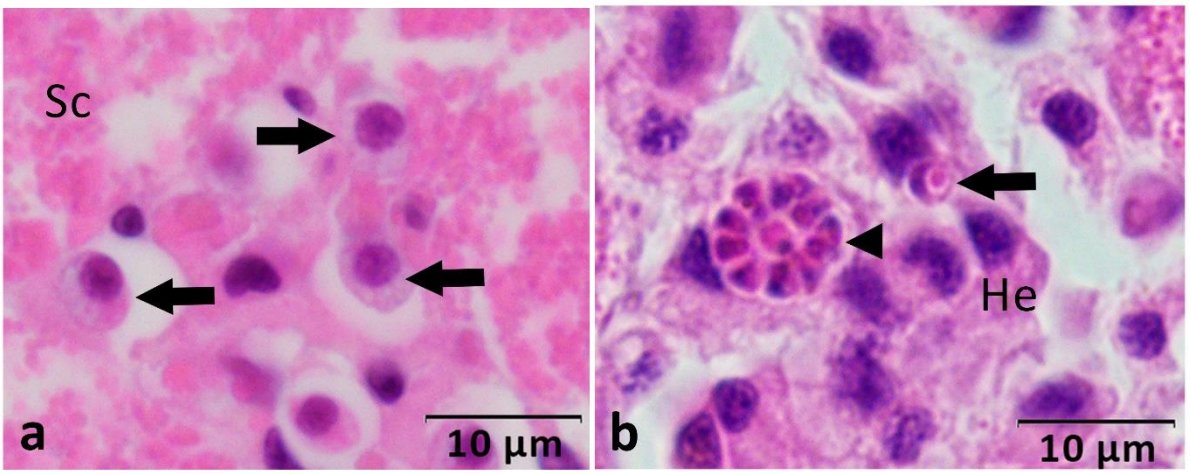

Figure 9. *APX* and *Perkinsus olseni.* a) *APX* level 2: a group of 6 APX zoites within the mantle tissue no ceroid material or hemocytosis associated. b) *P. olseni* indicating level 3 displays different stages of the lifecycle trophozoite signet ring (arrow) and the rosette-like (arrowhead). *P.olseni* cells detectable across mantle and connective tissue of multiple tissues occasionally associated with hemocytosis.

Table 8. Population prevalence (%) of parasites found in the *P. canaliculus.* APX and *P. olseni* are excluded from this table and discuss in further detail below.

	Temperature		
	17°C	21°C	24°C
Endozoicomonas	0.0	1.6	1.9
Microsporidium rapuae	0.7	0.8	0.0
Paravortex	0.7	0.0	0.0

Copepod	2.1	1.6	2.9
Ciliates	1.4	0.0	0.0

APX was present in mussels in all three temperatures, and by month 4 of thermal exposure, APX approached 100% population prevalence. Small groups of APX were found scattered in the mantle, connective tissue of digestive glands and gut subepithelial as well as at the base of the gills and plicate organ near the kidney. Ceroid material was only associated occasionally at this level. No differences were identified among the sample time points, but a significant difference in the total population prevalence of APX was observed between mussels in the 17°C and 24°C temperatures with prevalence being higher in the 24°C treatment ($t = 2.548$, $p=0.011$). *P. olseni* detection in mussels increased with temperature between 24°C compared to 17°C temperatures ($t = 6.051$, $p <0.001$), and there was an interaction between temperature and time ($t = 4.058$, $p <0.001$). The first detection of *P. olseni* in mussels occurred in 24°C, 5 months after the start of thermal manipulation (i.e., month 7), which was 2 months earlier than detection in mussels at 21°C. *P. olseni* was detected in only 1 individual at 17°C towards the conclusion of the trial (Table 9). Focal hemocytosis (hemocytes - He) was associated to *P. olseni* cells.

Table 9. Population prevalence (%) of APX and *P. olseni* during 15 months of sampling at three temperatures 17°C, 21°C and 24°C (sample numbers available in Table 1)

		Sampling month														
		2b	**4**	**5**	**6**	**6b**	**7**	**8**	**9**	**10**	**11**	**12b**	**13**	**14**	**15**	**16b**
APX	**17°C**	33	75	63	25	100	100	100	100	100	100	100	100	100	100	100
	21°C		100	75	50	80	100	100	100	100	100	100	100	100	88	100
	24°C		100	88	88	100	100	100	100	75	88	100	88	100	100	
P. olseni	**17°C**	0	0	0	0	0	0	0	0	0	0	0	0	13	0	0
	21°C		0	0	0	0	0	0	13	0	13	0	13	38	25	17
	24°C		0	0	0	0	38	25	25	50	63	50	25	50	25	

The APX intensity levels throughout this trial were quite low and, as such, only the first three semi-quantitative grades from Hine (2002) and Suong (2018) were required. The average intensities of APX across the three temperatures were 17°C = 1.3 ± 0.6 (n=109), 21°C = 1.4 ± 0.5 (n=108) and 24°C = 1.1 ± 0.4 (n=90) (mean ± SD). The average intensity of *P. olseni* was relatively low at 17°C = 1 (n=1), 21°C = 2.1 ± 0.9 (n=11) and 24°C = 1.8 ± 0.8 (n=28) (mean

Pre-Proof

± SD). No lesions were identified in response to APX and minor hemocyte reactions were present on occasion with *P. olseni* (Fig. 9).

4. Discussion

Prolonged exposure to constant temperature, even at the benign 17°C typical in summer was associated with apparently deleterious histopathological alterations in digestive gland, gill and gonad (The artificial constancy of laboratory trials and its potential confounding effect is discussed in section 4.5). Higher temperatures and prolonged exposure were also associated with increased prevalence of the pathogen *Perkinsus olseni*, suspension of gametogenesis, and oocyte atresia (see below). Elevated temperatures, in addition, significantly impacted survival, growth and immune response as also reported by (Ericson et al., 2023). The histopathological alterations associated with elevated temperature may be valuable in assessing vulnerability to environmental challenges such as those arising with climate change. Further refinement of these potential indicators would contribute to improved health assessment of *P. canaliculus* and the aquaculture industry it supports.

4.1. Impacts on survival and growth.

In a complementary study, Ericson et al. (2023) demonstrated that for *P. canaliculus*, prolonged exposure to elevated temperatures (21°C and 24°C) was detrimental to both growth and survival. This detrimental effect indicates that the optimal thermal range was exceeded with consequential impacts on physiology, metabolism, immune response, and survival (Petes et al., 2007; Dame and Kenneth, 2011; Delorme et al., 2021). In addition, there was a noticeable difference in the development of byssus (anecdotal observation), where mussels at 24°C had sparse and weak byssus development compared with mussels maintained at lower temperatures Although not part of the initial experiment this is worth noting and exploring further in the future as mussels that prioritise growth, over byssal development in the natural environment (i.e. rocky shores) risk dislodgement and increased mortality (Clarke, 1999; Sebens et al., 2018; Roberts et al., 2021). The byssus threads were clipped four times throughout the trial to weigh and measure mussels, thus, introducing a potential confounding factor in terms of energy availability for growth, survival and immune response across all temperature treatments. The energetic cost of byssal production for reattachment therefore represented a compounding stressor for mussels within this study.

Pre-Proof

4.2. Tissue abnormalities

Chronic exposure to the three temperatures (17, 21 and 24°C) resulted in an accumulation of ceroid (lipofuscin-like pigment) during the course of the trial. The ceroid accumulation in response to thermal stress could be the result of an initial increase in metabolic rate, which leads to increased oxygen consumption, followed by higher basal reactive oxygen species (ROS) production, faster accumulation of peroxidised material and finally loss of cell function (see Ericson et al., 2023). Therefore, the accumulation of ceroid indicates accelerated senescence and potentially the advancement of the physiological age when compared with the chronological age (Terman and Brunk, 1998; Basova et al., 2012). Typically, lipofuscin production has been associated with aging and is also known to be a temperature dependent process Miquel et al. (1976); (e.g. in clams Lomovasky et al., 2002), whereas ceroid is considered to be a pigment associated to pathological conditions (Basova et al., 2012; Carella, 2015). There are several potential causes of ceroid accumulation, including immune response and oxidative stress (Zaroogian and Yevich, 1993). Increases in oxidative stress were observed in mussels exposed to the same temperature treatments in the complementary study by Ericson et al. (2023). Lipofuscin and ceroid are both end-products of lipid peroxidation and the oxidisation of proteins (Seehafer and Pearce, 2006; Basova et al., 2012; Carella, 2015), both also have the ability to catalyse their own formation and drive further lipid peroxidation (Jung et al. (2007). Due to the characteristic histological similarities between lipofuscin and ceroid material, it is difficult to determine the difference between the two in this work. Therefore, "ceroid" was used in this study to refer to the pigmented granules. Ceroid-lipofuscin accumulation has been considered to be an outcome of inadequate intra-lysosomal digestion from the phagocytosis process, these residual granules accumulate in the cell's cytoplasm, which can then be expelled into the connective tissue (Hendriks and Eestermans, 1986; Basova et al., 2012; Hartenstein and Martinez, 2019). . In addition, accumulation may also indicate previous and ongoing pathological conditions (i.e., APX and *Perkinsus sp*. exacerbating the accumulation).

Elevated recruitment of hemocytes to the gut region at higher temperatures may indicate defence against incoming pathogens or a response to altered gut microbiota and nutritional affects. For example, increased aggregations of hemocytes around the gut have been observed in *Crassostrea gigas* when exposed to the toxic algae *Alexandrium minutum* (Haberkorn et al., 2010). While hemocytes can function as defence cells, they also fulfil digestion and nutrient transport roles or support shell formation and tissue repair (e.g. Allam and Raftos, 2015; Rolton

Pre-Proof

and Ragg, 2020), the aggregation of hemocytes referred to as hemocytosis is a response limited to tissue repair and pathogens (see section 4.3) (e.g. Haberkorn et al., 2010; Ben-Horin et al., 2015). Across bivalve tissues, circulating hemocytes encapsulate and traffic pathogens such as viral particles through the gut epithelium (Haberkorn et al., 2010; Ben-Horin et al., 2015) in a process called diapedesis. This process has been suggested to be a defence response to protect the tissues (e.g. Haberkorn et al. (2010). The digestive process, gut epithelial layer and mucosal layers provide a strong defence against the physical environment and pathogens in healthy individuals. However, during host stress, such as the thermal stress inflicted here, physiological state and immunity may be compromised, allowing the entry of viruses, bacteria and parasites through the gut tract and pallial organs, such as the gills. (Bower, 2006; Ben-Horin et al., 2015).

In additional to minor alterations to the gill architecture there also appeared to be expression of the HSP70 protein with increasing temperature based on our preliminary observations. HSP70 is a wide spectrum heat inducible protein in the HSP family which is expressed under stress (Feder and Hofmann, 1999; Hu et al., 2022). Gills are directly exposed to the environment and therefore detection of HSP70 is not unexpected as a "first layer of defence" response to thermal stress. The increasing HSP70 expression with increasing temperature is worth further research as production is associated with a high energetic cost (Feder and Hofmann, 1999; Tomanek, 2010; Valenzuela-Castillo et al., 2019). Possibly though HSP70 production might have been beneficial for *P. canaliculus* exposed to higher temperatures, which could explain the minimal gill architectural alterations observed. The inclusion of these preliminary results is novel and promising for *P. canaliculus* and worth further investigation.

4.3. Pathogen prevalence and influence on the host

Perkinsus olseni was detected in mussels at month 7 at 24°C, month 9 at 21°C in the trial. The intensity of the parasite, based on (Hine and Diggles, 2002) and (Kim et al., 2006) was considered to be low and therefore potentially at the initial stage of infection. In association with *P. olseni*, there was an increasing intensity of focal hemocytosis at the elevated temperatures 21°C and 24°C. In addition, the presence of *P. olseni* was associated with decreased energy reserves and immune responses such as increased intensity of focal ceroid aggregations, focal hemocytosis, and encapsulation of parasites across different tissue types. The parasite is known to have an affinity for waters above 20°C which commonly occur in the North Island (Hine and Diggles, 2002) and the top of the South Island (Broekhuizen et al., 2021). This temperature (20°C) may represent a threshold of natural occurrence of *P. olseni* whereby infective cells are present in low concentrations in the environment, with temperatures

Pre-Proof

595 above this (e.g. 24°C from this research) accelerating initiation of infection (Lester, 1986;
596 Goggin and Lester, 1995). The present work corroborated this temperature effect.

597 Marine diseases are the result of complex host-parasite-environment interactions and there is
598 growing evidence to suggest that, in some cases, their increased prevalence and severity may
599 be associated with climate change (Harvell et al., 1999; Burge et al., 2014). Suboptimal
600 environmental conditions, such as temperature stress in combination with stressed hosts can
601 favour pathogen transmission and replication resulting in mortalities (Harvell et al., 1999).
602 *Perkinsus* sp. host interactions exemplify this. This protist endoparasite infects several species
603 worldwide including, Greenshell mussels, *Perna canaliculus* (Muznebin et al., 2022), the
604 clams *Austrovenus stutchburyi* (Dungan et al., 2007), *Paphies australis* (Ben-Horin et al.,
605 2015), abalone *Haliotis iris* (Hine and Diggles, 2002; Muznebin et al., 2021) and the oyster
606 *Crassostrea gigas* (Ben-Horin et al., 2015). Climate warming has been implicated in driving
607 increased spatial distribution of *Perkinsus* sp. and resulting disease events (Carella, 2015).

608 *Perkinsus* sp. inhibits phagocytosis and suppresses apoptosis of hemocytes in molluscs (OrdÁS
609 et al., 1999; Sunila and LaBanca, 2003; Hughes et al., 2010). Phagocytic inhibition allows the
610 parasites to infect and proliferate in circulating hemocytes, without being destroyed, and spread
611 to other tissues (e.g. OrdÁS et al., 1999; Sunila and LaBanca, 2003; Hughes et al., 2010; Ben-
612 Horin et al., 2015). Phagocytosis, is one of the main mechanisms for defence, it is a
613 temperature-dependent process (Oliver and Fisher, 1995) (Yu et al., 2009). The hemocytes in
614 the mussels at the warmer temperatures potentially tried to ingest the *P. olseni* cells initially,
615 without success. This process was then followed by parasite-mediated inhibition once infection
616 was established, with *Perkinsus* cells developing into replicative trophozoites. Partial
617 phagocytosing could have resulted in the inadequate intra-lysosomal digestion and therefore
618 further accumulation of ceroid material as described in the above section (Hendriks and
619 Eestermans, 1986; Hartenstein and Martinez, 2019).

620 As heatwaves progress, two outcomes are hypothesised, either pathogen intensity continues to
621 increase in response to favourable conditions, or the pathogen intensity diminishes allowing
622 for elimination in the host tissues during the cool winter months as previously suggested by
623 Goggin and Lester (1995). It remains a question of how *P. olseni* was acquired and whether
624 development to detectable levels was facilitated primarily by stress from the suboptimal
625 chronic conditions. In the current study, it was difficult to determine this or to establish the true
626 extent of the *P. olseni* infection, and whether *P. olseni* is detrimental to *P. canaliculus* and, if

Pre-Proof

so, at what intensity level. The occurrence of *P. olseni* was unexpected as it was not a pathogen-focused trial and, as such, this research highlights the need for additional surveillance methods and diagnostic tools including PCR and histology, when performing experiments. There is little published information regarding *P. canaliculus* as a host for *P. olseni* (Muznebin et al., 2022) and, considering that environmental fluctuations may be exacerbated by climate change, further research is required on the disease progression and implications for the Greenshell mussel industry and wild mussel beds. This should include work on farmed and wild populations to reflect conditions that are experienced in the sea.

The decline in energy reserves (glycogen) within the mantle, and potentially the digestive glands, is likely to explain the decline in *P. canaliculus* weight found by (Ericson et al., 2023) in response to elevated temperature (21 and 24°C). Additionally, the thermal stress and potentially the *P. olseni* infection, in combination, are likely to have resulted in the observed decline in mantle energy reserves from month 10 onward at 24°C. However declines in weight-based measurements, such as condition index have been observed in other mussels, such as *Mytilus edulis* (Clements et al., 2018) and *P. canaliculus* (Venter et al., In Prep) primarily in response to elevated temperatures. The energy available for growth, immune response and reproduction is acquired through food assimilation and is stored as lipids and glycogen within the mantle tissues, digestive glands, and muscle. These reserves are primarily used as energy over the winter period, as well as for gametogenesis (Bayne et al., 1982; Hummel et al., 1989; Fearman et al., 2009). Accumulation and use of reserve glycogen content is likely to vary with environmental changes, such as extreme temperatures, pollution and starvation (Hummel et al., 1989). Glycogen is the primary carbohydrate used for maintenance under stressful conditions and has been used as an indicator of health (Bayne, 1976; Barber and Blake, 1981). The depletion of glycogen in storage cells is of interest and possibly related to several factors, including its allocation to processes, such as routine metabolic maintenance, shell and byssal development, phagocytosis and immune responses, as well its appropriation by pathogens (Cheng, 1983).

4.4. Reproductive condition

Histopathological investigations in this study have revealed that at initial sampling timepoints, *P. canaliculus* mussels were passing the ripe and spawning stage and advancing towards the post-spawning, spent stage. Prolonged experimental exposure, irrespective of temperature, was observed to have impacts on reproductive condition in the present study. Gametogenesis was suspended with increased atresia (oocyte degradation) in the majority of the mussels in all

Pre-Proof

660 temperature treatments, including the "benign" 17°C, which may result from a) the prolonged
661 temperature stress, b) without the quiescent winter phase, the initiation of gonadogenesis is
662 indistinguishable, regardless of the amount of food available, c) reproduction is the first
663 energetic process to be sacrificed when temperatures are outside the reproductive optimum and
664 d) an undetected mussel spawning occurred post-transfer into the system prior to trial initiation.

665 Successful reproduction is crucial for the survival of any species. It is an energy-demanding
666 process with its own physiological stressors. It has been found that sublethal conditions in the
667 environment can inhibit reproduction as many species will reallocate energy from gamete
668 production and move it to the somatic tissues for growth, defence and repair (Michalek-Wagner
669 and Willis, 2001; Petes et al., 2007). Heat shock proteins are one of the main defence and repair
670 mechanisms in organisms (Feder and Hofmann, 1999; Tomanek, 2010; Valenzuela-Castillo et
671 al., 2019). In this study, a seemingly higher HSP70 expression was observed in gonads of
672 mussels exposed to elevated temperatures, indicating that the mussels had activated specific
673 mechanisms to cope with the stress; as has been shown in other marine invertebrates (e.g. Nash
674 et al., 2019; Delorme et al., 2020a; Delorme et al., 2020b). Additionally, the HSP70 presence
675 in gonad tissue suggests that mussels responded to the heat stress by investing in loading the
676 gametes with HSP70 to protect their offspring against potential further increases in temperature
677 or other stressors. As a result of the promising preliminary observations further research and
678 targeted sampling is required to determine the mechanisms of parental investment in *P.*
679 *canaliculus* exposed to chronic heat stress.

680 The lack of noticeable spawning and increased oocyte atresia observed within this investigation
681 suggests a potential strategy of *P. canaliculus* to cope with prolonged stress and may indicate
682 a method of adaptation and survival. Atresia is the degeneration and reabsorption of oocytes
683 prior to a spawning event and is a strategy to recycle energy (Beninger, 2017; Chérel and
684 Beninger, 2017). Atresic oocytes are determined by their histological characterisations and
685 unusual fixation effects, such as shrunken, highly irregular shapes, cytoplasmic detachment
686 from membrane, lysing of the membrane and increased staining affinity (Beninger, 2017;
687 Chérel and Beninger, 2017). Atresia has been reported in a number of bivalve species, e.g. the
688 clam *Tapes philippinarum* (Chérel and Beninger, 2017), oyster *Crassostrea gigas* (Steele and
689 Mulcahy, 1999) and mussels *Mytilus edulis* (Pipe, 1987), *Mytilus galloprovincialis* (Ortiz-
690 Zarragoitia et al., 2011) and *Aulacomya atra* (Pérez et al., 2013). The probable causes of
691 increased incidence and intensities of atresia are adverse environmental conditions, including
692 pollution, starvation, and sub-optimal temperature (Galap et al., 1997; Steele and Mulcahy,

Pre-Proof

1999; Pérez et al., 2013; Vazquez et al., 2020). Atresia is a strategy to reallocate energy reserves in order to cope with stress and energy depletion (Beninger, 2017). Observations of atresia in this study are therefore expected, particularly when *P. canaliculus* were exposed to sub-optimal high temperatures. Furthermore, the incidence of atresia prior to increasing the temperatures was higher than expected and is of interest. Several questions remain for example, was the incidence of atresia at this point representative of field conditions or a result of reallocation of energy to byssal development following stripping from the farm ropes at initial collection time? additionally was the atresia due to movement into the spent stage as a result of an undetected spawning resulting in an additional stressor as well as a loss of energy. Failure to identify and determine atresia within field and the laboratory populations will result in several implications including over-estimations of fecundity and reproductive effort (Beninger, 2017).

Both reproduction and somatic growth reflect complex intrinsic and extrinsic interactions. The reproductive cycle is controlled by both endogenous factors and environment, with temperature being the driving force behind the initiation and the rate of gametogenesis (Michalek-Wagner and Willis, 2001; Petes et al., 2007). Reproductive timing, synchronicity, fertilisation, and recruitment success are influenced by temperature. Chronic stress can lead to a loss of propagules, low gamete quality and spawning of pre-mature gametes that supply the adult population (Walther et al., 2002; Philippart et al., 2003; Petes et al., 2007; Petes et al., 2008). *P. canaliculus* is a dioecious broadcast spawning species with gonadal development and gametogenesis occurring throughout the year (Alfaro et al., 2001; Buchanan, 2001). The depletion of the glycogen content and the decline in growth (Ericson et al., 2023) in *P. canaliculus* exposed to elevated temperatures during the present study suggests there is very little residual energy after increased metabolism for both growth and reproduction, as observed in other molluscan species (Fearman and Moltschaniwskyj, 2010). Present and future climate change influences on environmental stressors are of major concern for *P. canaliculus* in the aquaculture industry and in the wild. In terms of reproductive capability, it is crucial to determine the true extent of oocyte atresia in *P. canaliculus* and how ongoing stressors, such as marine heatwaves are likely to impact oocyte development further. Knowledge relating to interactions between the reproductive condition and health of *P. canaliculus* is key for the aquaculture industry, particularly as heatwaves increase in frequency and intensity (Beninger, 2017). Such expected changes to reproduction and spawning status of mussels could impact the aquaculture industry by affecting not only their ability to plan harvesting operations, but their ability to produce economically valuable products.

Pre-Proof

4.5. Research implications

It was surprising that the unchanging conditions within this study were ultimately detrimental and 17°C, although considered as a benign temperature, does have negative effects over time. This impact on overall health in the benign treatment was also observed in the immune stress indicators in the complementary study by Ericson et al. (2023). It is yet to be determined whether these effects on the benign temperature was due to captivity stressors, including nutrition, density effects, lack of natural variation, and general holding conditions, although, a similar effect of capitivity has been considered and observed in other invertebrates such as mytilids (Bayne and Thompson, 1970) and freshwater mussels (Roznere et al., 2021; Morin et al., 2022). The thermal conditions in this study were maintained to eliminate treatment variability and focus on temperature as a single stressor. Single stressor long-term studies such as the work present herein are required to isolate the compounding effects of continuous stress such as temperature elevations. While *P. canaliculus* mussels in their natural environment are unlikely to be chronically exposed to elevated temperatures for the extended durations used in this study the average sea surface temperatures are increasing. Although, predictions of climate change are highly complex, impacts of increasing seawater temperatures on species phenology, distribution and physiological performance are likely (Zippay and Helmuth, 2012; Shelmerdine et al., 2017; Steeves et al., 2018). Therefore, the results of this work provide key knowledge on health at a tissue level and caution is required when extrapolating laboratory data to field conditions.

4.6. Conclusions

The present research identified changes in response to thermal stress and provides new insights into the host-environment-pathogen interactome for *P. canaliculus* under changing environments. Additionally, this is the first study that shows immunodetection of HSP70 in *P. canaliculus*. The decline in growth, loss of byssal development and suspension of gametogenesis in *P. canaliculus* suggests that, with increasing temperature and loss of seasonal variability, there is insufficient energy available after metabolic maintenance and immune defence in the laboratory conditions provided. In addition, the unexpected appearance of *P. olseni* needs further investigation and could be indicative of potential range spread if average temperatures and marine heatwave frequency continue to rise. Although, the HSP 70 technique is not comprehensively studied within this research it is a novel technique for this species, the small numbers of samples that were selected for IHC, do show promising protein expression

Pre-Proof

between temperature treatments in the gills and gonad and is worth future investigation. Furthermore, the aetiological causes of the mortalities during the trial are also still to be determined, with further investigations required to determine whether the mortalities were a result of exhaustion of energy reserves, phagocytosis inhibition, increased toxicity in the tissues from anaerobic metabolism, increased toxicity from the ceroid accumulation or other causes. Timely sampling at point of death before decay had set in would have provided further information for this investigation. This work highlights the potential effects of chronic thermal stress if climate change and marine heatwave frequency continues to rise**.** Further work using simultaneous laboratory and field studies incorporating realistic fluctuating and increased temperatures, as well as baseline ambient sampling, will help to provide further beneficial knowledge on the future impacts to *P. canaliculus* in response to climate change.

Acknowledgements:

We would like to give huge thanks to the technical staff at Cawthron Institute for the ongoing maintenance and monitoring of the trial as well as the Aquaculture Biotechnology Research Group at the Auckland University of technology for their support. We thank Lizenn Delisle and Paula Casanovas for their ongoing support, and Rodney Roberts for his review and comments. Lastly, we thank SPATnz for providing the Greenshell mussels used in this experiment, Medlab Central Histopathology, Palmerston North, for their assistance with histology processing and the Hugh Green Foundation for their ongoing support and funding of the Hugh Green Cytometry Centre. This research was supported and funded by the New Zealand Ministry for Business, Innovation and Employment, through the Cawthron Shellfish Aquaculture Research Platform (Contract CAWX1801) and the Aquatic Animal Health Programme (CAWX1707).

5. References

Alfaro, A.C., Jeffs, A.G., Hooker, S.H., 2001. Reproductive behavior of the green-lipped mussel, *Perna canaliculus*, in Northern New Zealand. Bulletin of Marine Science 69, 1095-1108

Alfaro, A.C., Young, T., 2018. Showcasing metabolomic applications in aquaculture: a review. Reviews in Aquaculture 10, 135-152

Pre-Proof

Allam, B., Raftos, D., 2015. Immune responses to infectious diseases in bivalves. J Invertebr Pathol 131, 121-136, 'doi'10.1016/j.jip.2015.05.005.

Angilletta Jr, M.J., Angilletta, M.J., 2009. Thermal adaptation: a theoretical and empirical synthesis.

Barber, B.J., Blake, N.J., 1981. Energy storage and utilization in relation to gametogenesis in *Argopecten irradians concentricus* (Say). Journal of Experimental Marine Biology and Ecology 52, 121-134

Basova, L., Begum, S., Strahl, J., Sukhotin, A., Brey, T., Philipp, E., Abele, D., 2012. Age-dependent patterns of antioxidants in *Arctica islandica* from six regionally separate populations with different lifespans. Aquatic Biology 14, 141-152

Bayne, B., 1976. Marine mussels, their ecology and physiology. Cambridge University Press, Cambridge

Bayne, B., Bubel, A., Gabbott, P., Livingstone, D., Lowe, D., Moore, M., 1982. Glycogen utilisation and gametogenesis in *Mytilus edulis* L. Marine Biology Letters 3

Bayne, B.L., Thompson, R.J., 1970. Some physiological consequences of keeping *Mytilus edulis* in the laboratory. Helgoländer Wissenschaftliche Meeresuntersuchungen 20, 526-552, 'doi'10.1007/bf01609927.

Behrens, E., Rickard, G., Rosier, S., Williams, J., Morgenstern, O., Stone, D., 2022. Projections of Future Marine Heatwaves for the Oceans Around New Zealand Using New Zealand's Earth System Model. Frontiers in Climate 4, 'doi'10.3389/fclim.2022.798287.

Ben-Horin, T., Bidegain, G., Huey, L., Narvaez, D.A., Bushek, D., 2015. Parasite transmission through suspension feeding. Journal of Invertebrate Pathology 131, 155-176

Beninger, P.G., 2017. Caveat observator: the many faces of pre-spawning atresia in marine bivalve reproductive cycles. Marine Biology 164, 163, 'doi'10.1007/s00227-017-3194-x.

Bignell, J.P., Dodge, M.J., Feist, S.W., Lyons, B., Martin, P.D., Taylor, N.G.H., Stone, D., Travalent, L., Stentiford, G.D., 2008. Mussel histopathology: effects of season, disease and species. Aquatic Biology 2, 1-15, 'doi'10.3354/ab00031.

Bower, S.M., 2006. Synopsis of infectious diseases and parasites of commercially exploited shellfish: Ciliates associated with Abalone. dfo,https://www.dfo-mpo.gc.ca/science/aah-saa/diseases-maladies/ciliatesab-eng.html.

Boyd, P.W., Lennartz, S.T., Glover, D.M., Doney, S.C., 2014. Biological ramifications of climate-change-mediated oceanic multi-stressors. Nature Climate Change 5, 71-79, 'doi'10.1038/nclimate2441.

Pre-Proof

Broekhuizen, N., Plew, D.R., Pinkerton, M.H., Gall, M.G., 2021. Sea temperature rise over the period 2002–2020 in Pelorus Sound, New Zealand – with possible implications for the aquaculture industry. New Zealand Journal of Marine and Freshwater Research 55, 46-64, 'doi'10.1080/00288330.2020.1868539.

Buchanan, S., 2001. Measuring reproductive condition in the Greenshell™ mussel *Perna canaliculus*. New Zealand Journal of Marine and Freshwater Research 35, 859-870, 'doi'10.1080/00288330.2001.9517048.

Burge, C.A., Mark Eakin, C., Friedman, C.S., Froelich, B., Hershberger, P.K., Hofmann, E.E., Petes, L.E., Prager, K.C., Weil, E., Willis, B.L., Ford, S.E., Harvell, C.D., 2014. Climate change influences on marine infectious diseases: implications for management and society. Ann Rev Mar Sci 6, 249-277, 'doi'10.1146/annurev-marine-010213-135029.

Carella, F.F., S.W. Bignell, J.P. DeVico G. , 2015. Comparative pathology in bivalves: Etiological agents and disease processes. Journal of Invertebrate Pathology 131, 13

Cheng, T.C., 1983. The role of lysosomes in molluscan inflammation. American Zoologist 23, 129-144

Chérel, D., Beninger, P.G., 2017. Oocyte Atresia Characteristics and Effect on Reproductive Effort of Manila Clam *Tapes philippinarum* (Adams and Reeve, 1850). Journal of Shellfish Research 36, 549-557, 'doi'10.2983/035.036.0302.

Chong, R.S.-M., 2022. Molluscan immunology, in: Kibenge, F.S.B., Baldisserotto, B., Chong, R.S.-M. (Eds.), Aquaculture Pathophysiology. Academic Press, pp. 383-392,10.1016/b978-0-323-95434-1.00057-7.

Clarke, M., 1999. The effect of food availability on byssogenesis by the zebra mussel (*Dreissena polymorpha Pallas*). Journal of Molluscan Studies 65, 327-333, 'doi'10.1093/mollus/65.3.327.

Clements, J.C., Hicks, C., Tremblay, R., Comeau, L.A., 2018. Elevated seawater temperature, not pCO(2), negatively affects post-spawning adult mussels (*Mytilus edulis*) under food limitation. Conserv Physiol 6, cox078, 'doi'10.1093/conphys/cox078.

Costa, P.M., 2018. Introduction, in: Costa, P.M. (Ed.), The Handbook of Histopathological Practices in Aquatic Environments. Academic Press, pp. 1-20,10.1016/b978-0-12-812032-3.00001-0.

Cule, E.S., Frankowski, M.D., 2021. ridge: Ridge Regression with Automatic Selection of the Penalty Parameter. R package version 3.0, https://CRAN.R-project.org/package=ridge

Dame, R.F., Kenneth, M.J., 2011. Ecology of marine bivalves: an ecosystem approach. Taylor & Francis,10.1201/b11220.

Pre-Proof

Dawber, C., Association, N.Z.M.F., Staff, N.Z.M.F.A., 2004. Lines in the water: A history of greenshell mussel farming in New Zealand. River Press

de la Ballina, N.R., Maresca, F., Cao, A., Villalba, A., 2022. Bivalve Haemocyte Subpopulations: A Review. Frontiers in Immunology 13, 826255, 'doi'10.3389/fimmu.2022.826255.

Delorme, N., Biessy, L., South, P., Zamora, L., Ragg, N., Burritt, D., 2020a. Stress-on-stress responses of a marine mussel, *Perna canaliculus*: food limitation reduces the ability to cope with heat stress in juveniles. Marine Ecology Progress Series 644, 105-117

Delorme, N.J., Frost, E.J., Sewell, M.A., 2020b. Effect of acclimation on thermal limits and hsp70 gene expression of the New Zealand sea urchin *Evechinus chloroticus*. Comp Biochem Physiol A Mol Integr Physiol 250, 110806, 'doi'10.1016/j.cbpa.2020.110806.

Delorme, N.J., Venter, L., Rolton, A., Ericson, J.A., 2021. Integrating animal health and stress assessment tools using the green-lipped mussel *Perna canaliculus* as a case study. Journal of Shellfish Research 40, 93-112

Dungan, C.F., Reece, K.S., Moss, J.A., Hamilton, R.M., Diggles, B.K., 2007. *Perkinsus olseni* in vitro isolates from the New Zealand clam *Austrovenus stutchburyi*. J Eukaryot Microbiol 54, 263-270, 'doi'10.1111/j.1550-7408.2007.00265.x.

Dunphy, B.J., Ragg, N.L., Collings, M.G., 2013. Latitudinal comparison of thermotolerance and HSP70 production in F2 larvae of the greenshell mussel (*Perna canaliculus*). Journal of Experimental Biology 216, 1202-1209, 'doi'10.1242/jeb.076729.

Dunphy, B.J., Ruggiero, K., Zamora, L.N., Ragg, N.L.C., 2018. Metabolomic analysis of heat-hardening in adult green-lipped mussel (*Perna canaliculus*): A key role for succinic acid and the GABAergic synapse pathway. Journal of Thermal Biology 74, 37-46, 'doi'https://doi.org/10.1016/j.jtherbio.2018.03.006.

Dunphy, B.J., Watts, E., Ragg, N.L.C., 2015. Identifying Thermally-Stressed Adult Green-Lipped Mussels (*Perna canaliculus* Gmelin, 1791) via Metabolomic Profiling. American Malacological Bulletin 33, 127-135, 129

Ericson, J.A., Venter, L., Copedo, J.S., Nguyen, V.T., Alfaro, A.C., Ragg, N.L.C., 2023. Chronic heat stress as a predisposing factor in summer mortality of mussels, *Perna canaliculus*. Aquaculture 564, 'doi'10.1016/j.aquaculture.2022.738986.

Fearman, J.-A., Bolch, C.J.S., Moltschaniwskyj, N.A., 2009. Energy storage and reproduction in mussels, *Mytilus galloprovincialis*: The influence of diet quality. Journal of Shellfish Research 28, 305-312, 308

Pre-Proof

Fearman, J., Moltschaniwskyj, N., 2010. Warmer temperatures reduce rates of gametogenesis in temperate mussels, *Mytilus galloprovincialis*. Aquaculture 305, 20-25

Feder, M.E., Hofmann, G.E., 1999. Heat-shock proteins, molecular chaperones, and the stress response: evolutionary and ecological physiology. Annu Rev Physiol 61, 243-282, 'doi'10.1146/annurev.physiol.61.1.243.

Filgueira, R., Guyondet, T., Comeau, L.A., Tremblay, R., 2016. Bivalve aquaculture-environment interactions in the context of climate change. Global Change Biology 22, 3901-3913, 'doi'10.1111/gcb.13346.

Fulda, S., Gorman, A.M., Hori, O., Samali, A., 2010. Cellular stress responses: cell survival and cell death. Int J Cell Biol 2010, 214074, 'doi'10.1155/2010/214074.

Galap, C., Leboulenger, F., Grillot, J.P., 1997. Seasonal variations in biochemical constituents during the reproductive cycle of the female dog cockle *Glycymeris glycymeris*. Marine Biology 129, 625-634, 'doi'10.1007/s002270050205.

Galinou-Mitsoudi, S., Sinis, A.I., 1994. Reproductive Cycle and Fecundity of the Date Mussel *Lithophaga Lithophaga* (Bivalvia: Mytilidae). Journal of Molluscan Studies 60, 371-385, 'doi'10.1093/mollus/60.4.371.

Garrabou, J., Coma, R., Bensoussan, N., Bally, M., ChevaldonnÉ, P., Cigliano, M., Diaz, D., Harmelin, J.G., Gambi, M.C., Kersting, D.K., Ledoux, J.B., Lejeusne, C., Linares, C., Marschal, C., PÉRez, T., Ribes, M., Romano, J.C., Serrano, E., Teixido, N., Torrents, O., Zabala, M., Zuberer, F., Cerrano, C., 2009. Mass mortality in Northwestern Mediterranean rocky benthic communities: effects of the 2003 heat wave. Global Change Biology 15, 1090-1103, 'doi'10.1111/j.1365-2486.2008.01823.x.

Goggin, C., Lester, R., 1995. *Perkinsus*, a protistan parasite of abalone in Australia: a review. Marine and Freshwater Research 46, 639-646

Gosling, E., 2008. Bivalve molluscs: biology, ecology and culture. John Wiley & Sons

Haberkorn, H., Lambert, C., Le Goïc, N., Moal, J., Suquet, M., Guéguen, M., Sunila, I., Soudant, P., 2010. Effects of *Alexandrium minutum* exposure on nutrition-related processes and reproductive output in oysters *Crassostrea gigas*. Harmful Algae 9, 427-439, 'doi'10.1016/j.hal.2010.01.003.

Hadfield, J.D., 2010. MCMC Methods for Multi-Response Generalized Linear Mixed Models: TheMCMCglmmRPackage. Journal of Statistical Software 33, 1 - 22, 'doi'10.18637/jss.v033.i02.

Pre-Proof

Hartenstein, V., Martinez, P., 2019. Phagocytosis in cellular defense and nutrition: a food-centered approach to the evolution of macrophages. Cell Tissue Res 377, 527-547, 'doi'10.1007/s00441-019-03096-6.

Harvell, C.D., Kim, K., Burkholder, J.M., Colwell, R.R., Epstein, P.R., Grimes, D.J., Hofmann, E.E., Lipp, E.K., Osterhaus, A.D., Overstreet, R.M., Porter, J.W., Smith, G.W., Vasta, G.R., 1999. Emerging marine diseases--climate links and anthropogenic factors. Science 285, 1505-1510, 'doi'10.1126/science.285.5433.1505.

Hendriks, H.R., Eestermans, I.L., 1986. Phagocytosis and lipofuscin accumulation in lymph node macrophages. Mech Ageing Dev 35, 161-167, 'doi'10.1016/0047-6374(86)90006-0.

Hine, M., Diggles, B., 2002. The distribution of *Perkinsus olseni* in New Zealand bivalve molluscs. Surveillance (Wellington) 29, 8-11

Hine, P.M., 2002. Severe apicomplexan infection in the oyster *Ostrea chilensis*: a possible predisposing factor in bonamiosis. Dis Aquat Organ 51, 49-60, 'doi'10.3354/dao051049.

Hobday, A.J., Alexander, L.V., Perkins, S.E., Smale, D.A., Straub, S.C., Oliver, E.C.J., Benthuysen, J.A., Burrows, M.T., Donat, M.G., Feng, M., Holbrook, N.J., Moore, P.J., Scannell, H.A., Sen Gupta, A., Wernberg, T., 2016. A hierarchical approach to defining marine heatwaves. Progress in Oceanography 141, 227-238, 'doi'10.1016/j.pocean.2015.12.014.

Hooper, C., Day, R., Slocombe, R., Benkendorff, K., Handlinger, J., Goulias, J., 2014. Effects of severe heat stress on immune function, biochemistry and histopathology in farmed Australian abalone (hybrid *Haliotis laevigata*×*Haliotis rubra*). Aquaculture 432, 26-37, 'doi'10.1016/j.aquaculture.2014.03.032.

Houghton, J.E.T., Ding, Y., Griggs, D., Noguer, M., van der Linden, P., Dai, X., Maskell, M., Johnson, C., 2001. Climate Change 2001: The Scientific Basis: Contribution of Working Group I to the Third Assessment Report of the Intergovernmental Panel on Climate Change (IPCC). Cambridge University Press, p. 881

Howard, D.W., 2004. Histological techniques for marine bivalve mollusks and crustaceans. NOAA, National Ocean Service, National Centers for Coastal Ocean Service, Center for Coastal Environmental Health and Biomolecular Research,, Cooperative Oxford Laboratory

Hu, Z., Song, H., Feng, J., Zhou, C., Yang, M.-J., Shi, P., Yu, Z.-L., Li, Y.-R., Guo, Y.-J., Li, H.-Z., Zhang, T., 2022. Massive Heat Shock Protein 70 Genes Expansion and Transcriptional Signatures Uncover Hard Clam Adaptations to Heat and Hypoxia. Frontiers in Marine Science 9, 'doi'10.3389/fmars.2022.898669.

Pre-Proof

954 Hughes, F.M., Foster, B., Grewal, S., Sokolova, I.M., 2010. Apoptosis as a host defense
955 mechanism in *Crassostrea virginica* and its modulation by *Perkinsus marinus*. Fish &
956 Shellfish immunology 29, 247-257
957 Hummel, H., de Wolf, L., Zurburg, W., Apon, L., Bogaards, R.H., van Ruitenburg, M., 1989.
958 The glycogen content in stressed marine bivalves: The initial absence of a decrease.
959 Comparative Biochemistry and Physiology Part B: Comparative Biochemistry 94, 729-733,
960 'doi'10.1016/0305-0491(89)90157-0.
961 Jeffs, A.G., Holland, R.C., Hooker, S.H., Hayden, B.J., 1999. Overview and Bibliography of
962 research on the Greenshell Mussel, *Perna canaliculus*, from New Zealand waters. Journal of
963 Shellfish Research 18, 347-360
964 Jung, T., Bader, N., Grune, T., 2007. Lipofuscin: formation, distribution, and metabolic
965 consequences. Ann N Y Acad Sci 1119, 97-111, 'doi'10.1196/annals.1404.008.
966 Kennedy, V.S., 2010. Reproduction in *Mytilus edulis aoteanus* and *Aulacomya maoriana*
967 (Mollusca: Bivalvia) from Taylors mistake, New Zealand. New Zealand Journal of Marine
968 and Freshwater Research 11, 255-267, 'doi'10.1080/00288330.1977.9515676.
969 Kim, Y., Ashton-Alcox, K.A., Powell, E.N., 2006. Histological techniques for marine bivalve
970 molluscs: update. NOAA/National Centers for Coastal Ocean Science
971 King, P.A., McGrath, D., Gosling, E.M., 2009. Reproduction and Settlement of *Mytilus*
972 *edulis* on an Exposed Rocky Shore in Galway Bay, West Coast of Ireland. Journal of the
973 Marine Biological Association of the United Kingdom 69, 355-365,
974 'doi'10.1017/s0025315400029465.
975 Knowles, G., Handlinger, J., Jones, B., Moltschaniwskyj, N., 2014. Hemolymph chemistry
976 and histopathological changes in Pacific oysters (*Crassostrea gigas*) in response to low
977 salinity stress. J Invertebr Pathol 121, 78-84, 'doi'10.1016/j.jip.2014.06.013.
978 Law, C.S., Rickard, G.J., Mikaloff-Fletcher, S.E., Pinkerton, M.H., Behrens, E., Chiswell,
979 S.M., Currie, K., 2017. Climate change projections for the surface ocean around New
980 Zealand. New Zealand Journal of Marine and Freshwater Research 52, 309-335,
981 'doi'10.1080/00288330.2017.1390772.
982 Lester, R., 1986. Abalone die-back caused by protozoan infection? Australian Fisheries 45,
983 26-27
984 Li, S., Alfaro, A.C., Nguyen, T.V., Young, T., Lulijwa, R., 2020. An integrated omics
985 approach to investigate summer mortality of New Zealand Greenshell™ mussels.
986 Metabolomics 16, 1-16

Pre-Proof

Lomovasky, B.J., Morriconi, E., Brey, T., Calvo, J., 2002. Individual age and connective tissue lipofuscin in the hard clam *Eurhomalea exalbida*. Journal of Experimental Marine Biology and Ecology 276, 83-94, 'doi'10.1016/s0022-0981(02)00240-x.

Lubchenco, J., Navarette, S., Tissot, B., Castilla, J.C., 1993. Lubchenco, J. L., S. A. Navarette, B. N. Tissot, and J. C. Castilla. 1993. Possible ecological responses to global climate change: nearshore benthic biota of northeastern Pacific coastal ecosystems. Chapter 12 In: H. A. Mooney, E. R. Fuentes, and B. I. Kronberg. eds. Earth System Responses to Global Change: Contrasts between North and South America. Academic Press, San Diego,

Manduzio, H., Rocher, B., Durand, F., Galap, C., Leboulenger, F., 2005. The point about oxidative stress in molluscs. Invertebrate Survival Journal 2, 91-104

Michalek-Wagner, K., Willis, B.L., 2001. Impacts of bleaching on the soft coral Lobophytum compactum . I. Fecundity, fertilization and offspring viability. Coral Reefs 19, 231-239, 'doi'10.1007/s003380170003.

Miquel, J., Lundgren, P.R., Bensch, K.G., Atlan, H., 1976. Effects of temperature on the life span, vitality and fine structure of *Drosophila melanogaster*. Mech Ageing Dev 5, 347-370, 'doi'10.1016/0047-6374(76)90034-8.

Mooney, H., Larigauderie, A., Cesario, M., Elmquist, T., Hoegh-Guldberg, O., Lavorel, S., Mace, G.M., Palmer, M., Scholes, R., Yahara, T., 2009. Biodiversity, climate change, and ecosystem services. Current Opinion in Environmental Sustainability 1, 46-54, 'doi'10.1016/j.cosust.2009.07.006.

Morin, M., Jönsson, M., Wang, C.K., Craik, D.J., Degnan, S.M., Degnan, B.M., 2022. Crown-of-thorns starfish in captivity experience sustained large-scale changes in gene expression. bioRxiv, 2022.2007.2021.501052, 'doi'10.1101/2022.07.21.501052.

Muznebin, F., Alfaro, A.C., Webb, S.C., 2021. Occurrence of *Perkinsus olseni* and other parasites in New Zealand black-footed abalone (*Haliotis iris*). New Zealand Journal of Marine and Freshwater Research 57, 261-281, 'doi'10.1080/00288330.2021.1984950.

Muznebin, F., Alfaro, A.C., Webb, S.C., 2022. *Perkinsus olseni* and other parasites and abnormal tissue structures in New Zealand Greenshell™ mussels (*Perna canaliculus*) across different seasons. Aquaculture International 31, 547-582, 'doi'10.1007/s10499-022-00991-8.

Nash, S., Johnstone, J., Rahman, M.S., 2019. Elevated temperature attenuates ovarian functions and induces apoptosis and oxidative stress in the American oyster, *Crassostrea virginica*: potential mechanisms and signaling pathways. Cell Stress Chaperones 24, 957-967, 'doi'10.1007/s12192-019-01023-w.

Pre-Proof

Nguyen, T.V., Alfaro, A.C., 2020. Metabolomics investigation of summer mortality in New Zealand Greenshell mussels (Perna canaliculus). Fish Shellfish Immunol 106, 783-791, 'doi'10.1016/j.fsi.2020.08.022.

Oliver, E.C.J., Benthuysen, J.A., Bindoff, N.L., Hobday, A.J., Holbrook, N.J., Mundy, C.N., Perkins-Kirkpatrick, S.E., 2017. The unprecedented 2015/16 Tasman Sea marine heatwave. Nat Commun 8, 16101, 'doi'10.1038/ncomms16101.

Oliver, L., Fisher, W., 1995. Comparative form and function of oyster *Crassostrea virginica* hemocytes from Chesapeake Bay (Virginia) and Apalachicola Bay (Florida). Diseases of aquatic organisms 22, 217-225

OrdÁS, M.C., Novoa, B., Figueras, A., 1999. Phagocytosis inhibition of clam and mussel haemocytes by *Perkinsus atlanticus* secretion products. Fish & Shellfish Immunology 9, 491-503, 'doi'10.1006/fsim.1999.0208.

Ortiz-Zarragoitia, M., Garmendia, L., Barbero, M.C., Serrano, T., Marigomez, I., Cajaraville, M.P., 2011. Effects of the fuel oil spilled by the Prestige tanker on reproduction parameters of wild mussel populations. J Environ Monit 13, 84-94, 'doi'10.1039/c0em00102c.

Parmesan, C., Yohe, G., 2003. A globally coherent fingerprint of climate change impacts across natural systems. Nature 421, 37-42, 'doi'10.1038/nature01286.

Pawley, J., 2006. Handbook of biological confocal microscopy. Springer Science & Business Media

Perez-Cebrecos, M., Prieto, D., Blanco-Rayon, E., Izagirre, U., Ibarrola, I., 2022. Differential tissue development compromising the growth rate and physiological performances of mussel. Mar Environ Res 180, 105725, 'doi'10.1016/j.marenvres.2022.105725.

Pérez, A.F., Boy, C.C., Curelovich, J.N., Pérez Barros, P., Calcagno, J.Á., 2013. Relationship between energy allocation and gametogenesis in *Aulacomya atra* (Bivalvia: Mytilidae) in a sub-Antarctic environment. 48, 459-469

Petes, L.E., Menge, B.A., Murphy, G.D., 2007. Environmental stress decreases survival, growth, and reproduction in New Zealand mussels. Journal of Experimental Marine Biology and Ecology 351, 83-91

Petes, L.E., Mouchka, M.E., Milston-Clements, R.H., Momoda, T.S., Menge, B.A., 2008. Effects of environmental stress on intertidal mussels and their sea star predators. Oecologia 156, 671-680

Philippart, C.J., van Aken, H.M., Beukema, J.J., Bos, O.G., Cadée, G.C., Dekker, R., 2003. Climate-related changes in recruitment of the bivalve *Macoma balthica*. Limnology and Oceanography 48, 2171-2185

Pre-Proof

Pipe, R.K., 1987. Ultrastructural and cytochemical study on interactions between nutrient storage cells and gametogenesis in the mussel *Mytilus edulis*. Marine Biology 96, 519-528, 'doi'10.1007/bf00397969.

Portner, H.O., 2002. Climate variations and the physiological basis of temperature dependent biogeography: systemic to molecular hierarchy of thermal tolerance in animals. Comp Biochem Physiol A Mol Integr Physiol 132, 739-761, 'doi'10.1016/s1095-6433(02)00045-4.

Quinn, G.P., Keough, M.J., 2012. Experimental Design and Data Analysis for Biologists. Cambridge University Press, Cambridge,10.1017/cbo9780511806384.

R Core Team, 2021. R: A language and environment for statistical computing. R Foundation for Statistical Computing. Vienna, Austria, https://www.R-project.org/

Ren, J.S., Ragg, N.L.C., Cummings, V.J., Zhang, J., 2020. Ocean acidification and dynamic energy budget models: Parameterisation and simulations for the green-lipped mussel. Ecological Modelling 426, 109069, 'doi'10.1016/j.ecolmodel.2020.109069.

Ren, J.S., Ross, A.H., 2005. Environmental influence on mussel growth: A dynamic energy budget model and its application to the greenshell mussel *Perna canaliculus*. Ecological Modelling 189, 347-362, 'doi'10.1016/j.ecolmodel.2005.04.005.

Roberts, E.A., Newcomb, L.A., McCartha, M.M., Harrington, K.J., LaFramboise, S.A., Carrington, E., Sebens, K.P., 2021. Resource allocation to a structural biomaterial: Induced production of byssal threads decreases growth of a marine mussel. Functional Ecology 35, 1222-1239

Rolton, A., Ragg, N.L.C., 2020. Green-lipped mussel (*Perna canaliculus*) hemocytes: A flow cytometric study of sampling effects, sub-populations and immune-related functions. Fish Shellfish Immunol 103, 181-189, 'doi'10.1016/j.fsi.2020.05.019.

Roznere, I., Sinn, B.T., Daly, M., Watters, G.T., 2021. Freshwater mussels (Unionidae) brought into captivity exhibit up-regulation of genes involved in stress and energy metabolism. Sci Rep 11, 2241, 'doi'10.1038/s41598-021-81856-7.

RStudio Team, 2021. RStudio: Integrated Development Environment for R, RStudio, PBC

Rubio-Portillo, E., Izquierdo-Munoz, A., Gago, J.F., Rossello-Mora, R., Anton, J., Ramos-Espla, A.A., 2016. Effects of the 2015 heat wave on benthic invertebrates in the Tabarca Marine Protected Area (southeast Spain). Mar Environ Res 122, 135-142, 'doi'10.1016/j.marenvres.2016.10.004.

Salinger, M.J., Diamond, H.J., Behrens, E., Fernandez, D., Fitzharris, B.B., Herold, N., Johnstone, P., Kerckhoffs, H., Mullan, A.B., Parker, A.K., 2020a. Unparalleled coupled

Pre-Proof

ocean-atmosphere summer heatwaves in the New Zealand region: drivers, mechanisms and impacts. Climatic Change 162, 485-506

Salinger, M.J., Diamond, H.J., Behrens, E., Fernandez, D., Fitzharris, B.B., Herold, N., Johnstone, P., Kerckhoffs, H., Mullan, A.B., Parker, A.K., Renwick, J., Scofield, C., Siano, A., Smith, R.O., South, P.M., Sutton, P.J., Teixeira, E., Thomsen, M.S., Trought, M.C.T., 2020b. Unparalleled coupled ocean-atmosphere summer heatwaves in the New Zealand region: drivers, mechanisms and impacts. Climatic Change 162, 485-506, 'doi'10.1007/s10584-020-02730-5.

Salinger, M.J., Renwick, J., Behrens, E., Mullan, A.B., Diamond, H.J., Sirguey, P., Smith, R.O., Trought, M.C.T., Alexander, L., Cullen, N.J., Fitzharris, B.B., Hepburn, C.D., Parker, A.K., Sutton, P.J., 2019. The unprecedented coupled ocean-atmosphere summer heatwave in the New Zealand region 2017/18: drivers, mechanisms and impacts. Environmental Research Letters 14, 044023, 'doi'10.1088/1748-9326/ab012a.

Schindelin, J., Arganda-Carreras, I., Frise, E., Kaynig, V., Longair, M., Pietzsch, T., Preibisch, S., Rueden, C., Saalfeld, S., Schmid, B., Tinevez, J.Y., White, D.J., Hartenstein, V., Eliceiri, K., Tomancak, P., Cardona, A., 2012. Fiji: an open-source platform for biological-image analysis. Nat Methods 9, 676-682, 'doi'10.1038/nmeth.2019.

Sebens, K.P., Sara, G., Carrington, E., 2018. Estimation of fitness from energetics and life-history data: An example using mussels. Ecol Evol 8, 5279-5290, 'doi'10.1002/ece3.4004.

Seehafer, S.S., Pearce, D.A., 2006. You say lipofuscin, we say ceroid: defining autofluorescent storage material. Neurobiol Aging 27, 576-588, 'doi'10.1016/j.neurobiolaging.2005.12.006.

Seuront, L., Nicastro, K.R., Zardi, G.I., Goberville, E., 2019. Decreased thermal tolerance under recurrent heat stress conditions explains summer mass mortality of the blue mussel *Mytilus edulis*. Sci Rep 9, 17498, 'doi'10.1038/s41598-019-53580-w.

Shelmerdine, R.L., Mouat, B., Shucksmith, R.J., 2017. The most northerly record of feral Pacific oyster *Crassostrea gigas* (Thunberg, 1793) in the British Isles. BioInvasions Records 6, 57-60

Smale, D.A., Wernberg, T., Oliver, E.C.J., Thomsen, M., Harvey, B.P., Straub, S.C., Burrows, M.T., Alexander, L.V., Benthuysen, J.A., Donat, M.G., Feng, M., Hobday, A.J., Holbrook, N.J., Perkins-Kirkpatrick, S.E., Scannell, H.A., Sen Gupta, A., Payne, B.L., Moore, P.J., 2019. Marine heatwaves threaten global biodiversity and the provision of ecosystem services. Nature Climate Change 9, 306-312, 'doi'10.1038/s41558-019-0412-1.

Pre-Proof

1120 Steele, S., Mulcahy, M., 1999. Gametogenesis of the oyster *Crassostrea gigas* in southern
1121 Ireland. Journal of the Marine Biological Association of the United Kingdom 79, 673-686
1122 Steeves, L., Filgueira, R., Guyondet, T., Chassé, J., Comeau, L., 2018. Past, Present, and
1123 Future: Performance of Two Bivalve Species Under Changing Environmental Conditions.
1124 Frontiers in Marine Science 5, 184, 'doi'10.3389/fmars.2018.00184.
1125 Stenton-Dozey, J.M.E., Heath, P., Ren, J.S., Zamora, L.N., 2020. New Zealand aquaculture
1126 industry: research, opportunities and constraints for integrative multitrophic farming. New
1127 Zealand Journal of Marine and Freshwater Research 55, 265-285,
1128 'doi'10.1080/00288330.2020.1752266.
1129 Sunila, I., LaBanca, J., 2003. Apoptosis in the pathogenesis of infectious diseases of the
1130 eastern oyster *Crassostrea virginica*. Diseases of Aquatic Organisms 56, 163-170,
1131 'doi'10.3354/dao056163.
1132 Suong, N.T., Banks, J.C., Webb, S.C., Jeffs, A., Wakeman, K.C., Fidler, A., 2018. PCR test
1133 to specifically detect the apicomplexan 'X' (APX) parasite found in flat oysters *Ostrea*
1134 *chilensis* in New Zealand. Dis Aquat Organ 129, 199-205, 'doi'10.3354/dao03244.
1135 Sutton, P.J.H., Bowen, M., 2019. Ocean temperature change around New Zealand over the
1136 last 36 years. New Zealand Journal of Marine and Freshwater Research 53, 305-326,
1137 'doi'10.1080/00288330.2018.1562945.
1138 Terman, A., Brunk, U.T., 1998. Lipofuscin: mechanisms of formation and increase with age.
1139 APMIS 106, 265-276, 'doi'10.1111/j.1699-0463.1998.tb01346.x.
1140 Thomas, C.D., Cameron, A., Green, R.E., Bakkenes, M., Beaumont, L.J., Collingham, Y.C.,
1141 Erasmus, B.F., De Siqueira, M.F., Grainger, A., Hannah, L., Hughes, L., Huntley, B., Van
1142 Jaarsveld, A.S., Midgley, G.F., Miles, L., Ortega-Huerta, M.A., Peterson, A.T., Phillips, O.L.,
1143 Williams, S.E., 2004. Extinction risk from climate change. Nature 427, 145-148,
1144 'doi'10.1038/nature02121.
1145 Thomsen, M.S., Mondardini, L., Alestra, T., Gerrity, S., Tait, L., South, P.M., Lilley, S.A.,
1146 Schiel, D.R., 2019. Local Extinction of Bull Kelp (*Durvillaea* spp.) Due to a Marine
1147 Heatwave. Frontiers in Marine Science 6, 'doi'10.3389/fmars.2019.00084.
1148 Tomanek, L., 2010. Variation in the heat shock response and its implication for predicting the
1149 effect of global climate change on species' biogeographical distribution ranges and metabolic
1150 costs. J Exp Biol 213, 971-979, 'doi'10.1242/jeb.038034.
1151 Trump, B.F., Berezesky, I.K., Chang, S.H., Phelps, P.C., 1997. The pathways of cell death:
1152 oncosis, apoptosis, and necrosis. Toxicol Pathol 25, 82-88,
1153 'doi'10.1177/019262339702500116.

Pre-Proof

Tuckett, C.A., de Bettignies, T., Fromont, J., Wernberg, T., 2017. Expansion of corals on temperate reefs: direct and indirect effects of marine heatwaves. Coral Reefs 36, 947-956, 'doi'10.1007/s00338-017-1586-5.

Valenzuela-Castillo, A., Sánchez-Paz, A., Castro-Longoria, R., López-Torres, M.A., Grijalva-Chon, J.M., 2019. Hsp70 function and polymorphism, its implications for mollusk aquaculture: a review. Latin american journal of aquatic research 47, 224-231

Vazquez, N., Frizzera, A., Cremonte, F., 2020. Diseases and parasites of wild and cultivated mussels along the Patagonian coast of Argentina, southwest Atlantic Ocean. Dis Aquat Organ 139, 139-152, 'doi'10.3354/dao03467.

Venter, L., Alfaro, A., C, Ragg, N.L., C, Delorme, N.J., Ericson, J.A., In Prep. The effect of simulated marine heatwaves on green-lipped mussels, *Perna canaliculus*: A near-natural experimental approach.

Walther, G.R., Post, E., Convey, P., Menzel, A., Parmesan, C., Beebee, T.J., Fromentin, J.M., Hoegh-Guldberg, O., Bairlein, F., 2002. Ecological responses to recent climate change. Nature 416, 389-395, 'doi'10.1038/416389a.

Yu, J.H., Song, J.H., Choi, M.C., Park, S.W., 2009. Effects of water temperature change on immune function in surf clams, *Mactra veneriformis* (Bivalvia: Mactridae). J Invertebr Pathol 102, 30-35, 'doi'10.1016/j.jip.2009.06.002.

Zannella, C., Mosca, F., Mariani, F., Franci, G., Folliero, V., Galdiero, M., Tiscar, P.G., Galdiero, M., 2017. Microbial Diseases of Bivalve Mollusks: Infections, Immunology and Antimicrobial Defense. Mar Drugs 15, 182, 'doi'10.3390/md15060182.

Zaroogian, G., Yevich, P., 1993. Cytology and biochemistry of brown cells in *Crassostrea virginica* collected at clean and contaminated stations. Environmental Pollution 79, 191-197

Zippay, M.L., Helmuth, B., 2012. Effects of temperature change on mussel, *Mytilus*. Integr Zool 7, 312-327, 'doi'10.1111/j.1749-4877.2012.00310.x.

Pre-Proof